Summer 2014

Shielding effectiveness (SE) measurement for maxair waveguide panel, lossy material evaluation by laptop application

Xiao Li

Department:

SHIELDING EFFECTIVENESS (SE) MEASUREMENT FOR MAXAIR WAVEGUIDE PANEL, LOSSY MATERIAL EVALUATION BY LAPTOP APPLICATION

by

XIAO LI

A THESIS

Presented to the Faculty of the Graduate School of the

MISSOURI UNIVERSITY OF SCIENCE AND TECHNOLOGY

In Partial Fulfillment of the Requirements for the Degree

MASTER OF SCIENCE IN ELECTRICAL ENGINEERING

2014

Approved by

Victor Khilkevich, Advisor
James Drewniak
Alpesh Bhobe

ABSTRACT

The first part of the thesis presents the EM shielding effectiveness (SE) measurement of new kind of waveguide panel, MaxAir, which based on metal coating technology. SE Measurement tell the SE performance of MaxAir compared to the traditional metal waveguide panel. In terms of good features such as lower price, less weight, MaxAir could replace traditional waveguide panel in some applications by its SE results. There are two SE measurement methods are performed for MaxAir panel, both of them based on reverberation chamber. Measured SE for several MaxAir panel samples in different cell dimension and coating configuration. By the Measured SE results of MaxAir and simulated or measured results of pure metal traditional waveguide panel, MaxAir may not as good as traditional one, we need to trade off all of its features to meet the requirement of specific application.

The second part presents a measurement-based evaluation method for lossy material by laptop computer Wi-Fi application. The lossy material could help to reduce the EM noise from the internal components of laptop, which could affect the Wi-Fi communication. Then, based on this practical case, evaluate lossy material performance through the improvement of Wi-Fi behavior. Compared to traditional material property measurement, laptop Wi-Fi method could give a more intuitive evaluation results to how lossy material can help to improve electric product performance. In the measurement, build the Wi-Fi communication between two laptops, monitor the Wi-Fi performance when put material under test on the memory card socket. According to the data rate in different material case, some of lossy material can improve channel quality in the same noise condition.

ACKNOWLEDGMENTS

I would like to express my sincere gratitude not only to my advisor, Dr. Victor Khilkevich, but also to my former advisor, Dr. James Drewniak as well, for their constant encouragement, support and guidance throughout my master degree program. I want to thank Dr. Alpesh Bhobe, who help a lot for my internship work in CISCO. I also need to thank Dr. Jun Fan, Dr. David Pommerenke and Dr. Daryl Beetner for their guidance on my research work. I also want to thank all the EMC Lab students for their help.

I would like to thank my wife, Jing Li, for her love and selfless support in both my life and work throughout these years. I would also like to thank my family for their endless love and unconditional support during my study in US.

TABLE OF CONTENTS

LIST OF ILLUSTRATIONS

Page

LIST OF TABLES

Page

1 INTRODUCTION

Many apparatus and control rooms contain electronic equipment that is sensitive to external electromagnetic interference (EMI). The electronic equipment may also produce radiated energy that affects communications and measuring equipment in the near or far field environment [1]. Most typical waveguide panels are made of pure metal, such as steel or aluminum, which could provide the best electromagnetic (EM) shielding effectiveness (SE) performance in practice. Considering the trade-off between weight, cost, and SE of the panel, a new kind of metal coating, plastic-based waveguide panel (MaxAir) is developed.

The MaxAir panel, designed by the Laird Company, is a metal-plated plastic honeycomb panel with a conductive foam band around the perimeter. This panel is an alternative to the metal honeycomb vent panels used for EMI shielding, where efficient airflow is required [2]. Due to its lower cost and plastic based core material, the SE of MaxAir is not as good as a traditional panel and which also depends highly on the panel installation and edge treatment. Using simulation and measurement, we investigate an optimized configuration for panel installation to achieve MaxAir's best SE performance.

Several numerical methods can help calculate the SE of the infinite waveguide panel and a full-wave simulation run to obtain the SE results for different sizes of panel. Both methods would give accurate results [3]. These methods could apply on a typical waveguide panel, but not for MaxAir. Beside traditional analysis, we need to evaluate and study the MaxAir panel using measurement.

The measurement was based on the nested-cavity method, which is performed in a reverberation camber, and the setup considered same condition as the real application. By evaluating the MaxAir panel, we can ascertain the SE of MaxAir under different coating configurations, which is important for real applications. Moreover, we will find out how to improve the SE through the modification of the installation method.

In general terms, it is possible to describe the interaction of an EM wave with microwave absorbing materials as a phenomenon where the EM energy is transformed into thermal energy. According to the principle of energy conservation, an EM wave

impinging on a material can be reflected, attenuated, or transmitted through the material [4].

EMI has become a major issue in the field of electronics in the last few years, with higher and higher frequencies being used. The latest laptop computers have faster CPUs and memory. They communicate with each other through high-speed buses and there are powerful potential noise sources. Mutual interference may reduce their performance.

Many microwave sheets, absorbing materials, and evaluation methods give the accurate properties of the materials [13]. We can use an airline or waveguide to measure the dielectric and reflection factors of the absorbing material. However, for the real case, they cannot reflect the performance in a specific application directly. Product-based evaluation results give us a quick and instinctive understanding of the materials.

The noise from the fully running memory card could worsen the data channel between two laptops via a Wi-Fi connection, so when different absorbing materials are put in a certain place on a memory card, we can evaluate the material using the difference in channel quality. The most important issue for this method is to establish a stable and repeatable data channel between laptops to ensure reliable results for each absorbing material sample are obtained.

The paper has two parts. First, it reviews the basic structure of a waveguide panel and SE calculation, and then gives the detailed measurement methodology for the MaxAir panel using a reverberation chamber for the SE improvement. Second, we introduce the sheet absorbing material evaluation method using a laptop Wi-Fi application and present the measured results for different material samples.

2 SHIELDING EFFECTIVENESS MEASUREMENT OF MAXAIR WAVEGUIDE PANEL

2.1 INTRODUCTION OF WAVEGUIDE PANEL AND MAXAIR PANEL

The purpose of waveguide apertures is to improve the thermal environment for Processor Core Logic (PCL) components in chassis enclosures while enhancing EMI performance significantly. The PCL components consist of the processor, chipset, memory, and graphics components. To meet increasing thermal demands, the chassis must provide increased airflow and lower internal air temperatures. A typical chassis provides general EMI containment and cooling to the PCL components, but increasing thermal and EMI requirements require additional technology to facilitate this performance and maintain the balance between thermal and EMI performance. (Figure 2.1) shows an example of a panel containing an array of several waveguide apertures.

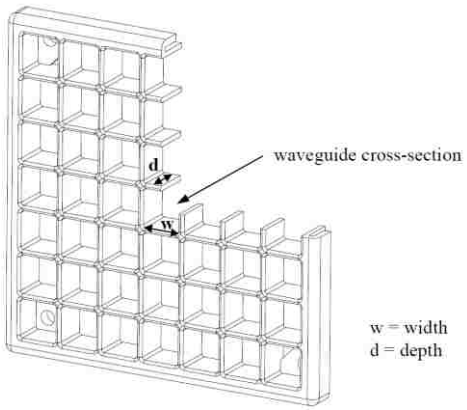

Figure 2.1 Example of waveguide panel/apertures

2.1.1. Principle of Waveguide Panel Operation. Waveguides are the most efficient way to transfer EM energy, however, EM shielding applications benefit from the 'disadvantages' of waveguides.

The physical size of a waveguide is their primary lower-frequency limitation. The

width of a waveguide must be approximately half the wavelength of the frequency of the wave to be transported. Waveguides are difficult to install because of their rigid, hollow-pipe shape. If the frequency of a signal is decreased so much that two quarter-wavelengths are longer than the wide dimension of a waveguide, energy will no longer pass through the waveguide. This is the lower frequency limit, or Cut-off Frequency. In other words, the cutoff frequency is the frequency beyond which the waveguide no longer effectively conduct EM wave. The inside dimensions of the waveguide determine this frequency.

We now assume that our "pipe" has a rectangular cross-section of dimensions a and b in the x and y directions, respectively (Figure 2.2). In the analysis to follow, we will actually prove this to, which supports the use of the above analysis for these waveguides. In a rectangular waveguide, the wave is not simply bouncing up and down in the y-z plane like the parallel plate waveguide. Certain waveguide modes can be thought of as bouncing off of all of the walls. Therefore, the electric and magnetic fields can have components in all three coordinate directions.

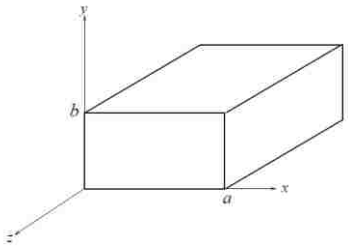

Figure 2.2 Rectangular wave guide dimension

The various modes are divided into two different cases in which either E_Z or H_Z is equal to zero. These two cases [1] are:

Transverse Electric (TE): The electric field is perpendicular to the propagation direction $\bar{E} \perp \hat{z}$ ($E_Z = 0$).

Transverse Magnetic (TM): The magnetic field is perpendicular to the propagation direction $\bar{H} \perp \hat{z}$ (H_Z = 0).

For both TE and TM modes, the wave number in the z direction could be Eq. (1):

$$k_z = \sqrt{k^2 - \left(\frac{m\pi}{a}\right)^2 - \left(\frac{n\pi}{b}\right)^2} \tag{1}$$

Notice that β depends on the frequency of operation mode numbers, m and n. For a given mode, if the frequency is such that β= 0, the mode does not propagate Eq. (2):

$$\beta^2 = k^2 - k_x^2 - k_y^2 = k^2 - k_c^2 = 0 \tag{2}$$

At this frequency, it is Eq. (3):

$$k = k_c = \sqrt{\left(\frac{m\pi}{a}\right)^2 + \left(\frac{n\pi}{a}\right)^2} \tag{3}$$

We call this condition cutoff. The value k_c is therefore the cutoff wavenumber. Using $k = \omega/c$, the cutoff frequency at which propagation stops for the TE_{mn} mode is Eq. (4).

$$f_{c,mn} = \frac{c}{2\pi}\sqrt{\left(\frac{m\pi}{a}\right)^2 + \left(\frac{n\pi}{a}\right)^2} \tag{4}$$

If the frequency of operation is below the cutoff frequency of the mode, so that $< f_{c,mn}$; then $k < k_c$ and $\beta = -j\alpha$ becomes imaginary. The z dependence of the mode then becomes $e^{-j\beta z} = e^{-\alpha z}$ so that the field decays in z. This is called an evanescent wave. So, for other waveguide shapes, such as circle or hexagon, the cutoff frequency could be calculated by a similar principle.

The waveguide panel is kind of array of many small waveguide ‘pipes’ (Figure 2.3), which could allow air or liquid flow go through the panel but prevent the EM signal below a certain frequency (Figure 2.4), this frequency is the cutoff frequency. As with the above definition, the cutoff frequency is only dependent on the cross-section dimension

of the waveguide cell of the panel, and the length of the cell will decide the signal attenuation.

Figure 2.3 Traditional waveguide panel

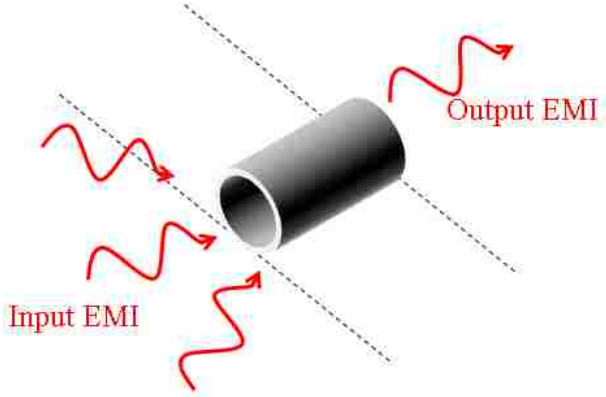

Figure 2.4 Basic waveguide operation

2.1.2. Features of Maxair Panel. The traditional waveguide is made of pure metal, such as steel or aluminum and has a very good EM shielding and mechanical performance, but the metal panel should cost higher than plastic panel, and heavier either. In some cases, the users do not need overqualified waveguide panels for their applications; they need something good enough in terms of both performance and price.

A new type of non-conductive material-based waveguide panel has been developed to meet the requirements above (Figure 2.5), the MaxAir panel, produced by the Laird Technology Company. The core material of this panel is polymer or plastic coated by a tiny layer of metal. The vent panel product line provides an innovative cost effective approach for providing increased airflow and EMI protection for telecommunications hardware equipment, such as fans and server racks. This nickel-copper plated polycarbonate honeycomb material provides a rigid medium, eliminating the need for costly frame designs. This frameless design allows greater airflow through the entire honeycomb surface and ease of installation through its press-to-fit assembly. The vent panel provides greater durability and flexibility than traditional pure metal vent panels.

Figure 2.5 Non-conductive material based vent panel

2.1.3. Typical Application of Honeycomb Panel in High-speed Network Equipment. The main purpose of the honeycomb panel is to prevent electric equipment from making EMI noise; however, it also needs to allow enough airflow through the electric components inside the equipment to cool them down (Figure 2.6). Modern high-speed network equipment, such as routers or switchers, are used for high-speed signal exchange and long distance signal transmission, so the honeycomb panel needs to work at high frequencies (up to 30GHz) and high power consumption (over 5kW). That means this network equipment has both a critical EMI and thermal problem. Therefore, the honeycomb panel should provide a suitable solution for that.

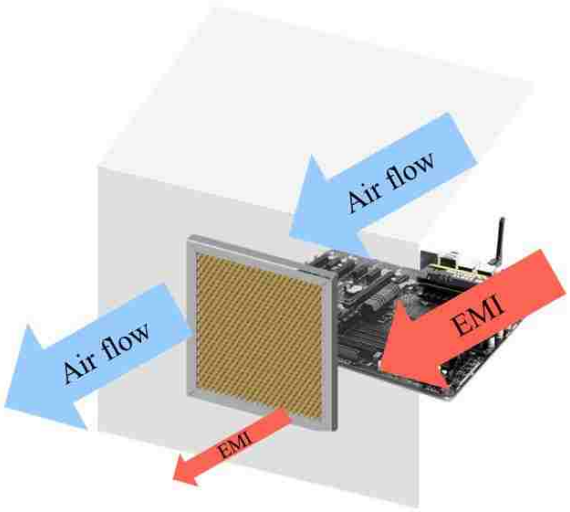

Figure 2.6 Function of honeycomb panel

For the EMI noise shielding, the PCB and components of the high performance switcher are enclosed in a metal chassis; in general, this kind of switcher includes sub-modules. Each module of switcher needs to be shielded by the EMI gaskets on the chassis. There are many ways for the air to flow, and these depend on the positions of honeycomb panel: rear-to-top, rear-to-bottom, sides-to-bottom, etc. (Figure 2.7). Some

high-level designs also use honeycomb panels to divide the chassis into several EMI-tight compartments to prevent the modules from mutual interference (Figure 2.8).

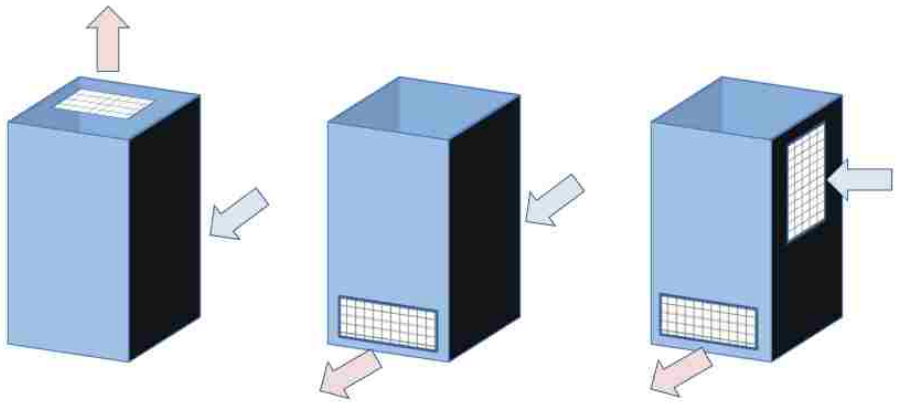

Figure 2.7 Honeycomb positions on the chassis

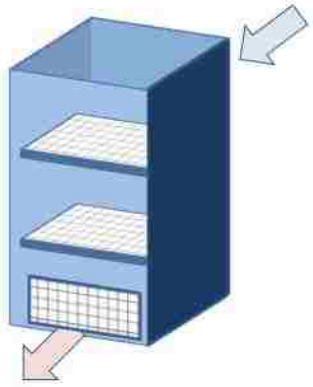

Figure 2.8 Chassis divided by honeycomb tray

The selection of the honeycomb is based on multiple elements that should be considered together: typical temperature inside the chassis, highest harmonic EM frequency, and highest power when equipment working. The cost is also important. The typical metal honeycomb could give an over-qualified performance but at a higher price.

A metal coating honeycomb like MaxAir could be installed on the front of each module or chassis because of its lighter weight (Figure 2.9), which could provide the shortest airflow path. On the other hand, the MaxAir is much cheaper than a traditional honeycomb panel, so it could replace the front panel of the chassis to maximize the cooling capacity.

Figure 2.9 MaxAir panel installed on front panel

From the SE measurement and study of the MaxAir panel, we would know the SE performance of different types of MaxAir panels, which helps to determine the specific applicable environment and to establish the installation method to make it perform better.

2.2 SHIELDING EFFECTIVENESS (SE) CALCULATION AND SIMULATION FOR WAVEGUIDE PANEL

In terms of theory of waveguide, we perform the numerical calculation for SE of the waveguide panel, and then validate the calculation results by full-wave EM simulation. Both numerical and simulation results could help the development and improvement of the coated vent panel.

2.2.1. SE Calculation of Infinite Waveguide Panel. As we already know the cutoff frequency of a single waveguide, the attenuation constant of guided waves is given as in the following approximated expression Eq. (5).

$$\alpha \approx \omega(\mu\varepsilon)^{\frac{1}{2}}\left[\left(\frac{f_c}{f}\right)^2 - 1\right]^{\frac{1}{2}} \tag{5}$$

Where f_c is the cutoff frequency of the waveguide.

Generally, there are three kinds of typical shape of waveguide: rectangular, circle, and hexagonal (Figure 2.10) and most vent panel structures are based on those shapes [5].

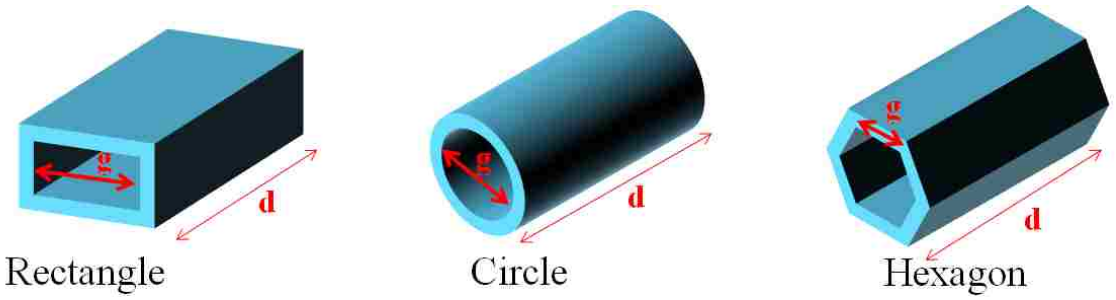

Figure 2.10 Typical shape of waveguide

Substituting the cut-off frequency into Eq. (5). this equation can be converted to an expression that is useful for estimating the attenuation constant in dB for a given conductor geometry. The equation of a rectangle, a circle, and a hexagon are summarized

in (Table 2.1). These equations are the SE for one cell of each waveguide. In the equations in (Table 2.1), d in mm is a waveguide length and g in mm is a transverse dimension of waveguide. f is the operating frequency in MHz [5].

Table 2.1 SE equations of different waveguide

	Rectangle	Circle	Hexagon
SE_{dB}	$SE_{dB} = 27.3\frac{d}{g}\sqrt{1-(\frac{gf}{150000})^2}$	$SE_{dB} = 31.95\frac{d}{g}\sqrt{1-(\frac{gf}{175800})^2}$	$SE_{dB} = 17.5\frac{d}{g}\sqrt{1-(\frac{gf}{96659})^2}$

As mentioned, the above equations are only for a single waveguide cell. When the cell is extended to all direction of its sides, it forms an infinite waveguide array or an infinite waveguide panel.

The Wiener–Hopf method analyzes the infinite array of waveguides [6]. The resulting equation Eq. (6) is shown below. The first term of the Eq. (6) is the SE of a unit cell of circle waveguide from (Table 2.1), while the second and third terms are the SE of an infinite array of parallel-plate waveguides [7].

$$SE_{dB} = 31.95\frac{d}{g}\sqrt{1-\left(\frac{gf}{175800}\right)^2} - 20log_{10}\frac{2kg}{\pi}cos\,\varphi + 20log_{10}\frac{2k_{cnm}g}{\pi}cos\,\varphi \qquad (6)$$

where, k is wavenumber, g is a transverse dimension of waveguide, and φ is an angle of an incident wave (Figure 2.11).

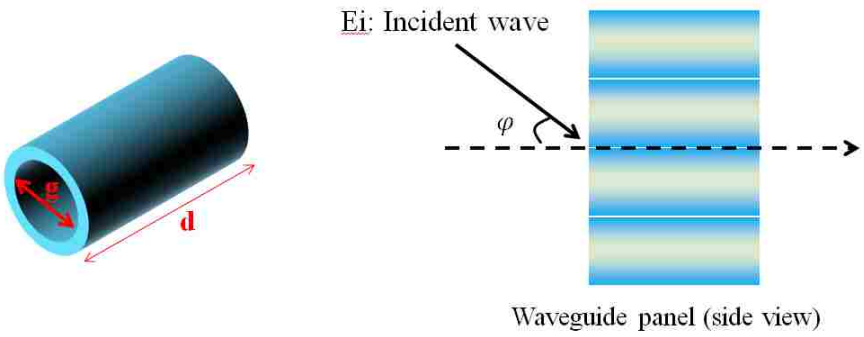

Figure 2.11 Parameter of circle waveguide

Therefore, we can calculate the SE of for an infinite circle waveguide panel according to Eq. (6), and the calculation results are shown in section 2.2.3 with the simulation results.

2.2.2. Shielding Effectiveness of Metal Sheet. For a metal-coated waveguide panel, the metal coating is too thin for the EM leakage to be ignored. Therefore, we need to consider the SE of the metal coating itself. The SE of a pure metal is highly dependent on the skin depth of the material, which should be taken into account when the thickness of the metal is thin enough.

When an EM wave propagating in one material encounters another material with different electrical properties, some of the energy in the wave is reflected and the rest is transmitted into the new material. Now consider a finite slab of shielding material illustrated in (Figure 2.1). An incident field, E_{inc}, strikes the surface of the shielding material. Some of the power in the field is reflected E_{ref} and some E_{slab} continues into the material. The part that penetrates the material is attenuated before it strikes the second surface at x = t. At that point, once again, some of the power is attenuated and some is transmitted.

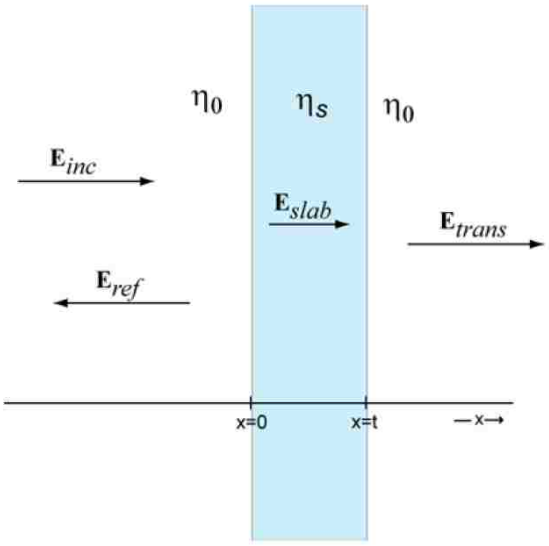

Figure 2.12 EM plane wave propagating in infinite metal material

If the attenuation is high, the power reflected at the second interface is absorbed and the field transmitted to the region of free space on the right of the slab is given by Eq. (7). where η_0 and η_s are the intrinsic impedance of the free space and the metal material, respectively.

$$|E_{trans}| = |E_{slab}(x = t)|T_{E_2} \tag{7}$$

Where

$$T_{E_2} = \frac{2\eta_s}{\eta_s+\eta_0} \tag{8}$$

$$|E_{slab}(x)| = |E_{slab}(x = 0)|e^{-\frac{x}{\delta}} \tag{9}$$

In Eq. (9), δ is the skin depth of the material. For high-loss materials:

$$\delta \approx \frac{1}{\sqrt{\pi f \mu \sigma}} \tag{10}$$

Combining Eq. (7), Eq. (8) and Eq. (9), we obtain an expression for the transmitted electric field in terms of the incident field Eq. (11).

$$|E_{trans}| = |E_{inc}| \frac{2\eta_s}{\eta_0+\eta_s}\left(\frac{2\eta_0}{\eta_0+\eta_s}\right) e^{-\frac{t}{\delta}} \tag{11}$$

If we define the shielding effectiveness of the slab to be Eq. (12):

$$SE = 20log\frac{E_{inc}}{E_{trans}} \tag{12}$$

Then in dB scale, the shielding effectiveness of an infinite sheet of good conductor can be written in the form Eq. (13):

$$SE(dB) = 20log\frac{\eta_0}{4\eta_s} + 20loge^{\frac{t}{\delta}} \tag{13}$$

Therefore, for the metal coating circle waveguide, we can assume that only one surface of the waveguide was coated is the worst case for SE, which could then give maximum leakage from the metal coating (Figure 2.13). Therefore, the total transmitted wave E_{trans} is not only from the waveguide penetration, but from the metal coating propagation as well. In (Figure 2.13),when the incident wave E_{in} is cast in the waveguide panel, some energy is reflected due to the property of the waveguide and some energy goes through the waveguide as E_{out}. Therefore, the rest of the energy will dwell in the waveguide as an input wave E_{in} for the metal coating.

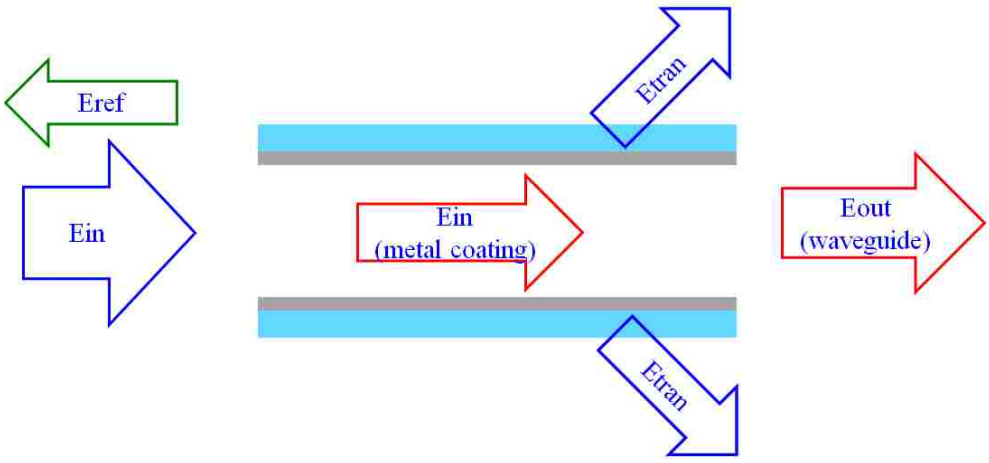

Figure 2.13 EM wave propagation in coated waveguide

In dB scale, the E_{out} could be Eq. (14). The remaining energy on the metal coating is Eq. (15), which also contribute the reflected wave of waveguide.

$$E_{out}(dB) = E_{in}(dB) - SE_{waveguide}(dB) \tag{14}$$

$$E_{in-metal\,sheet} = E_{in} - E_{out} \tag{15}$$

By the Eq. (13), Eq. (14), and Eq. (15), we could calculate transmit wave from the metal coating Eq. (16).

$$E_{tran}(dB) = E_{in-metal\,sheet}(dB) - SE_{metalsheet}(dB) \tag{16}$$

Then get the total shielding effectiveness of coated waveguide Eq. (17).

$$SE_{total}(dB) = E_{in}(dB) - (E_{tran} + E_{out})(dB) \tag{17}$$

Eq. (17) shows us the worst SE results of a coated waveguide panel. Referring to

Eq. (17) can help check and validate the measurement results of a certain configuration panel sample to obtain any possible problems of measurement method or setup. The calculation results for a panel sample are shown in section 2.2.3 with the simulation results.

2.2.3. SE Simulation for Infinite Waveguide Panel in CST. For the validation of a numerical calculation of a waveguide panel SE, we undertake a full-wave simulation using a time domain solver in CST. The model dimensions are shown in (Figure 2.14), here use periodic boundary condition to make waveguide extent infinitely to be an infinite waveguide array (Figure 2.15)(Figure 2.16).

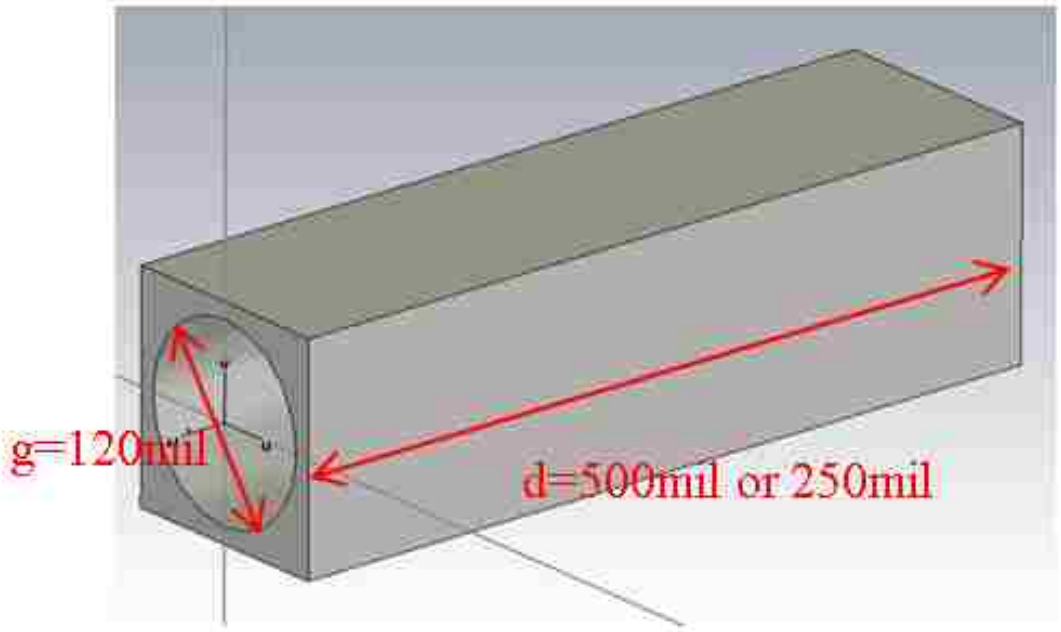

Figure 2.14 Waveguide model in CST

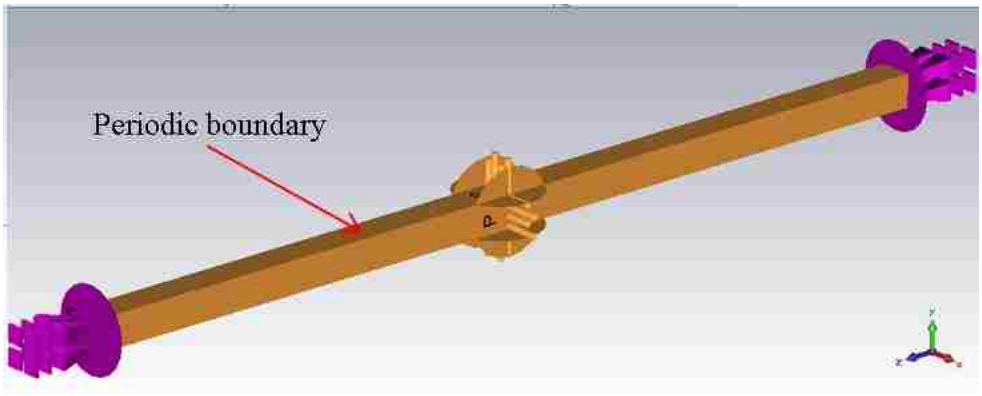

Figure 2.15 Boundary setting in CST

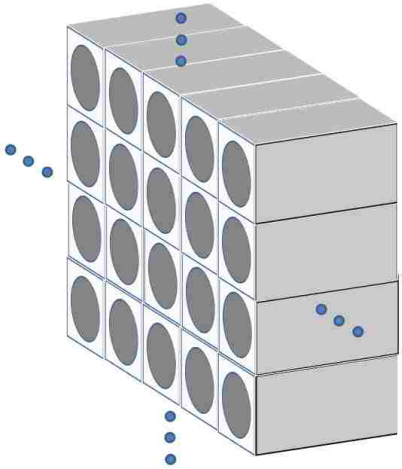

Figure 2.16 Waveguide array by periodic boundary

In CST, we build a small loop antenna as the EM wave excitation source for waveguide array, and this is 2000 mil away from the surface of the waveguide array (Figure 2.17). Then a discrete port excites that loop. Next, a magnetic field probe is set at the other side of the waveguide 500 mil away as a receiver. (Table 2.2) shows the simulation setting in the CST.

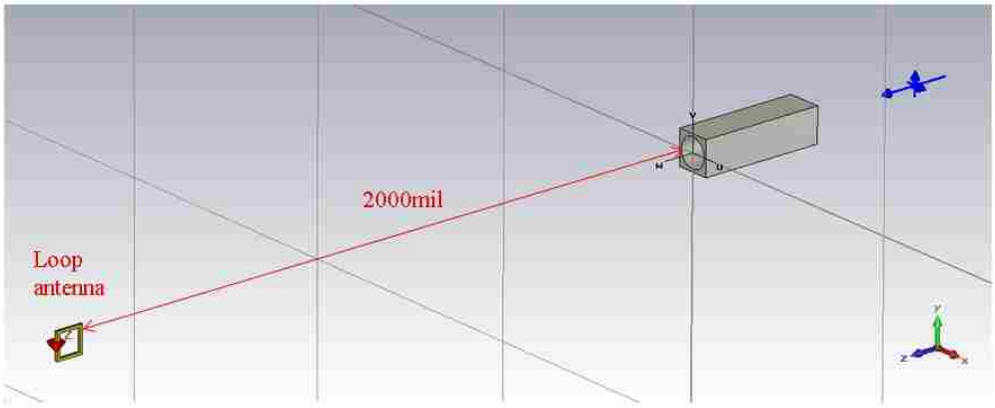

Figure 2.17 Simulation models in CST

Table 2.2 Simulation setting in CST

CST simulation setting	
Frequency	0GHz -20GHz, 20GHz – 50GHz
Boundary	Periodic
Loop antenna material	copper (lossy)
Waveguide material	PEC
Accuracy	-60dB
Mesh number:	176400

Firstly, the waveguide material is changed to ‘vacuum’, and then the magnetic field magnitude (H1) is obtained by using the probe. Next, the waveguide material is changed to ‘PEC’ and the simulation redone. The magnetic field is now H2. Therefore, in dB scale, the deviation of H1 and H2 is the SE of the waveguide array.

In terms of the dimensions in (Figure 2.14), the SE of the waveguide panel is calculated using Eq. (6) and calculated results compared with the simulation results, as (Figure 2.18) (Figure 2.19). From the comparison, the numerical calculation results agree with the simulated ones very well, meaning the equation is accurate enough to describe the SE performance of an infinite waveguide panel. From the simulation results, a ripple appeared along the curve due to the reflection between the loop antenna and the

waveguide panel, because the loop antenna is also a receiver when it is a source.

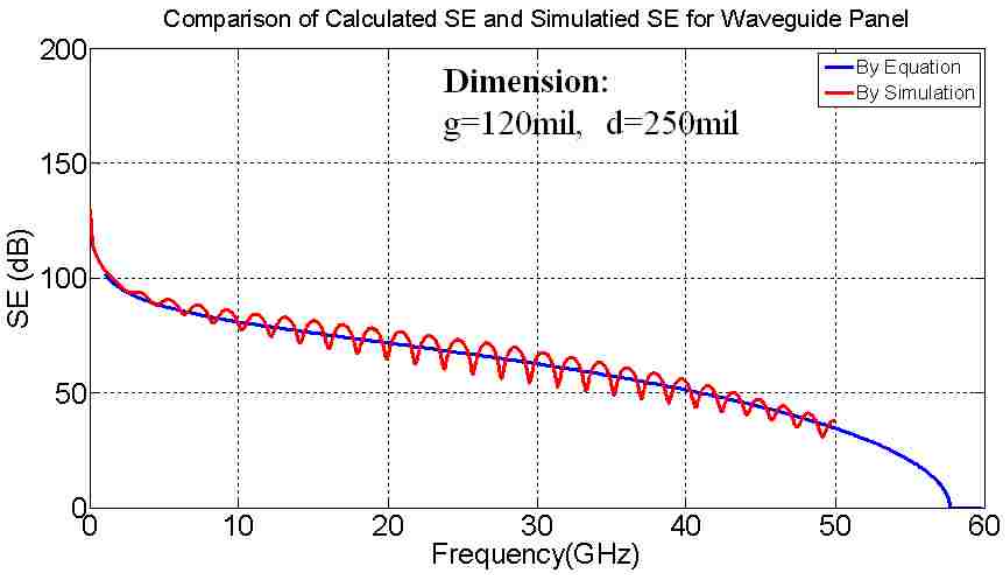

Figure 2.18 Comparison of simulation and calculation (250mil)

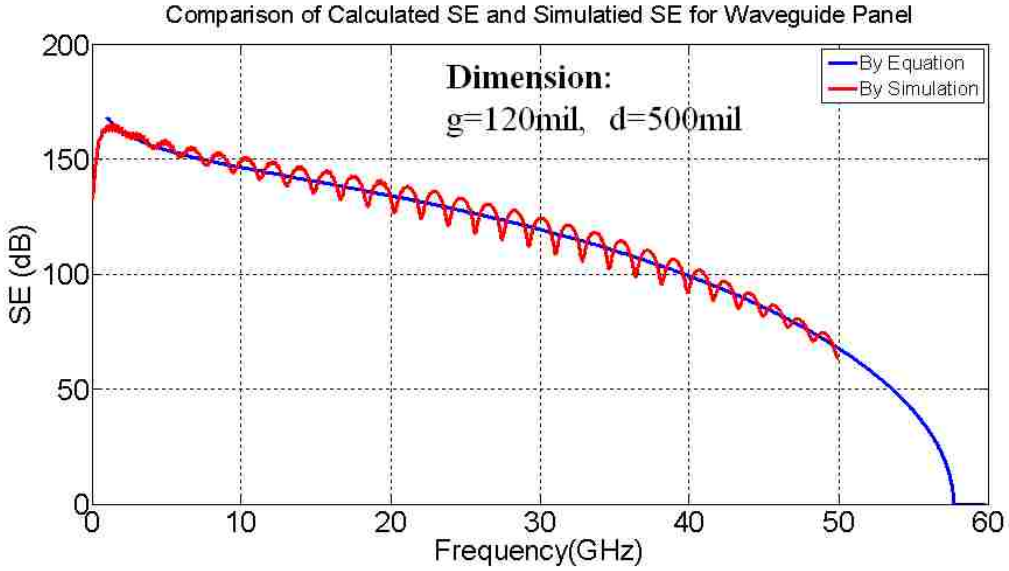

Figure 2.19 Comparison of simulation and calculation (500mil)

Both above results are for a traditional pure metal waveguide panel. If we consider the metal coating case (Figure 2.20), it is impossible to obtain accurate results from the full-wave simulation in CST when the dimensions of the metal are close to its skin depth. Therefore, we obtain approximate results from Eq. (17), as the predictable ones for coated panel.

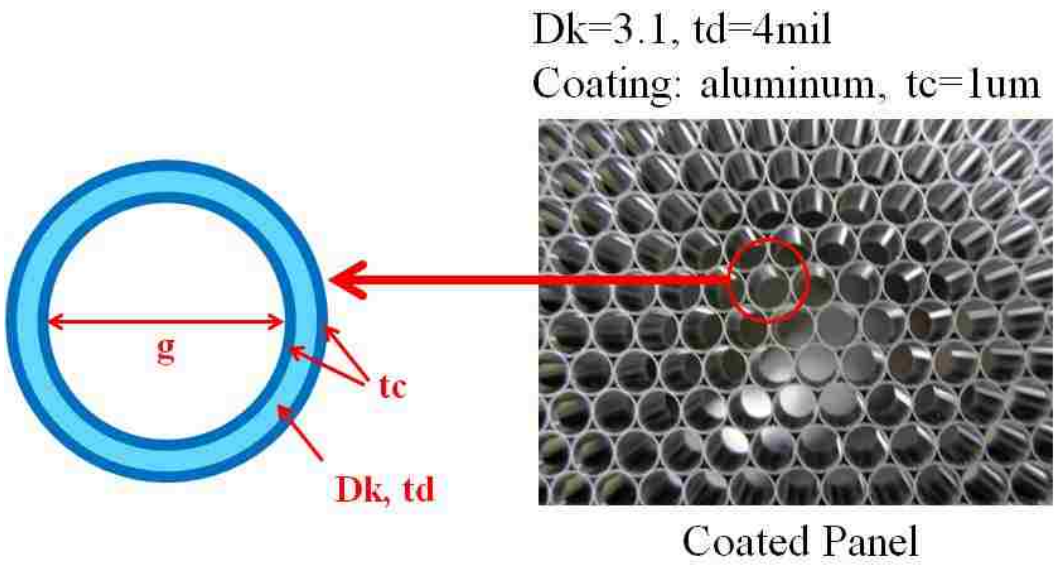

Figure 2.20 Metal coating waveguide panel

The calculated SE results of the coated waveguide panel are shown in (Figure 2.21) (Figure 2.22), which also compare with the results from the pure metal waveguide and pure metal sheet. We can see that the metal coating leakage of the coated panel SE is worse at a lower frequency.

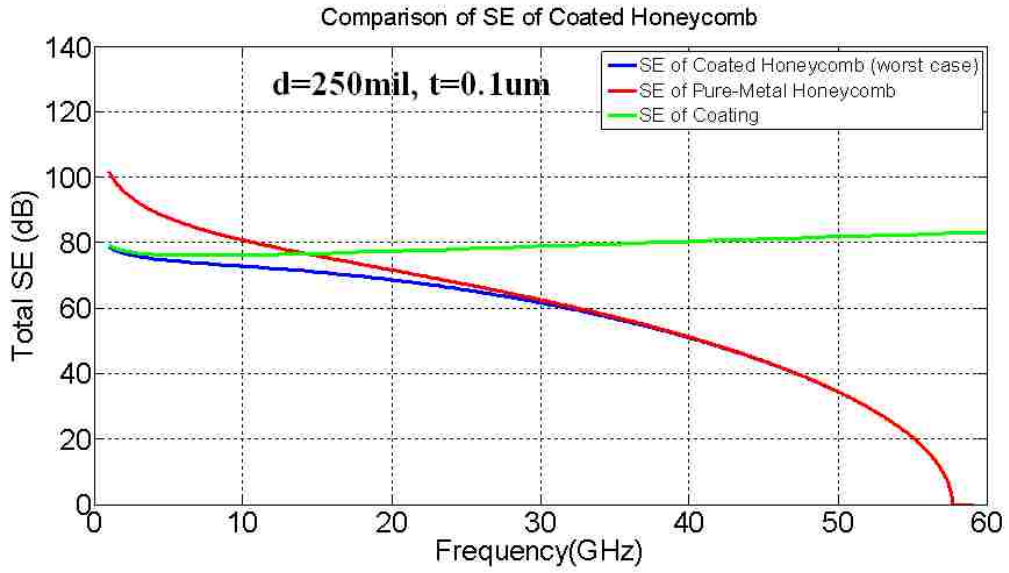

Figure 2.21 Coated panel SE result (250mil)

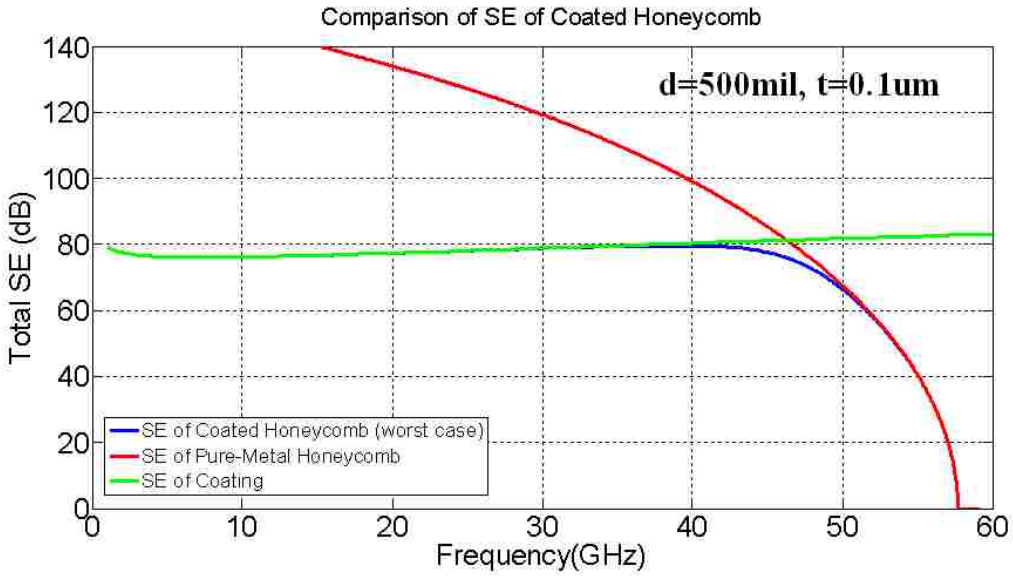

Figure 2.22 Coated panel SE result (500mil)

2.3 SE MEASUREMENT BY NESTED REVERBERATION CHAMBER BASED ON IEEE299

Besides the theoretical analysis of the waveguide panel SE, SE measurement also plays an important role in figuring out the SE property of a real waveguide panel sample;

to some extent, the measurement is more important than the simulation.

2.3.1. Introduction of Measurement Method. The SE measurement of a waveguide panel is based on the standard of IEEE 299.1, which defines the standard method for measuring the SE of enclosures and boxes with dimensions between 0.1 m and 2 m. This sub-section of IEEE 299.1 describes the basic test procedures for determining SE measurements. The approach is based on a nested reverberation chamber. A frequency-stirred reverberation chamber approach assumes that the enclosure is physically small (less than 0.75 m in the linear dimension), but electrically large. A diagram of the proposed approach is shown in (Figure 2.23).

The basic approach is to place the small enclosure in a reverberation chamber. This type of configuration is essentially a nested reverberation chamber as discussed in IEC 61000-5-7. In this setup, the source is placed inside the large reverberation chamber, and the reverberation chamber is sealed up. The source (e.g., horn connected to an RF signal generator) is then sweeped the frequency over a given frequency range. Since a portion of the RF energy in the outer chamber will couple into the small enclosure, this causes frequency stirring of the RF energy in the small enclosure. As a result, all points in the small enclosure statistically have the same field levels for the data averaged over some bandwidth of frequencies. Hence, the problem of sampling location is resolved without the need to have a paddle (or stirrer) in the small enclosure. The power levels in the small enclosure are monitored by a small monopole probe (or antenna) placed on one of the interior walls of the small enclosure. Thus, as long as the small enclosure is well stirred (i.e., through frequency-stirring), a small monopole probe placed on the inside wall will give the same average power level inside the small enclosure as that of an antenna placed in the center of the small enclosure. This frequency stirring in the outer chamber can be done with or without conventional mechanical stirring [8].

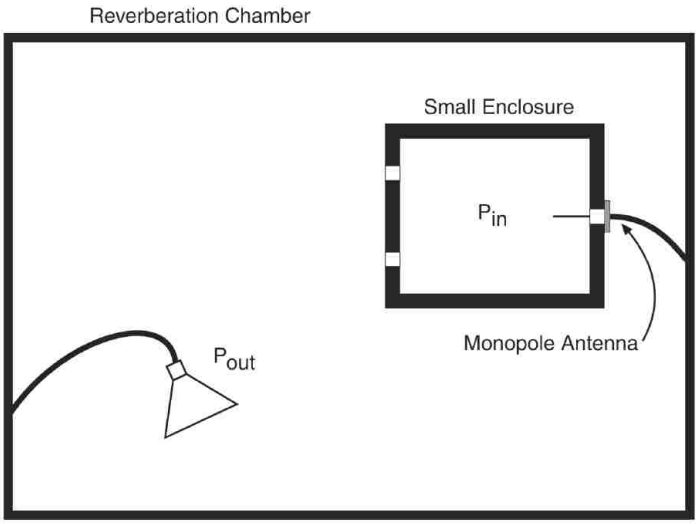

Figure 2.23 Illustration of the basic frequency-stirred reverberation chamber technique

The basic method for mathematically defining the shielding effectiveness of any enclosure is defined by Eq. (18).

$$SE = -10log_{10}(\frac{P_{in-close}}{P_{in-open}}) \quad (18)$$

Where $P_{in\text{-}close}$ and $P_{in\text{-}0pen}$ are the received power levels from monopole antenna inside with and without the small enclosure, respectively.

2.3.2. Measurement Setup and Data Processing. Based on the methods of IEEE 299.1, the SE test vehicle is setup for the waveguide panel. Using an EM shielded tent as a large reverberation chamber made of conductive fabric, a small enclosure is put in the tent as the nest of the waveguide panel. This aperture is the same size as the waveguide panel sample on the top of the small enclosure for panel sample installation (Figure 2.24).

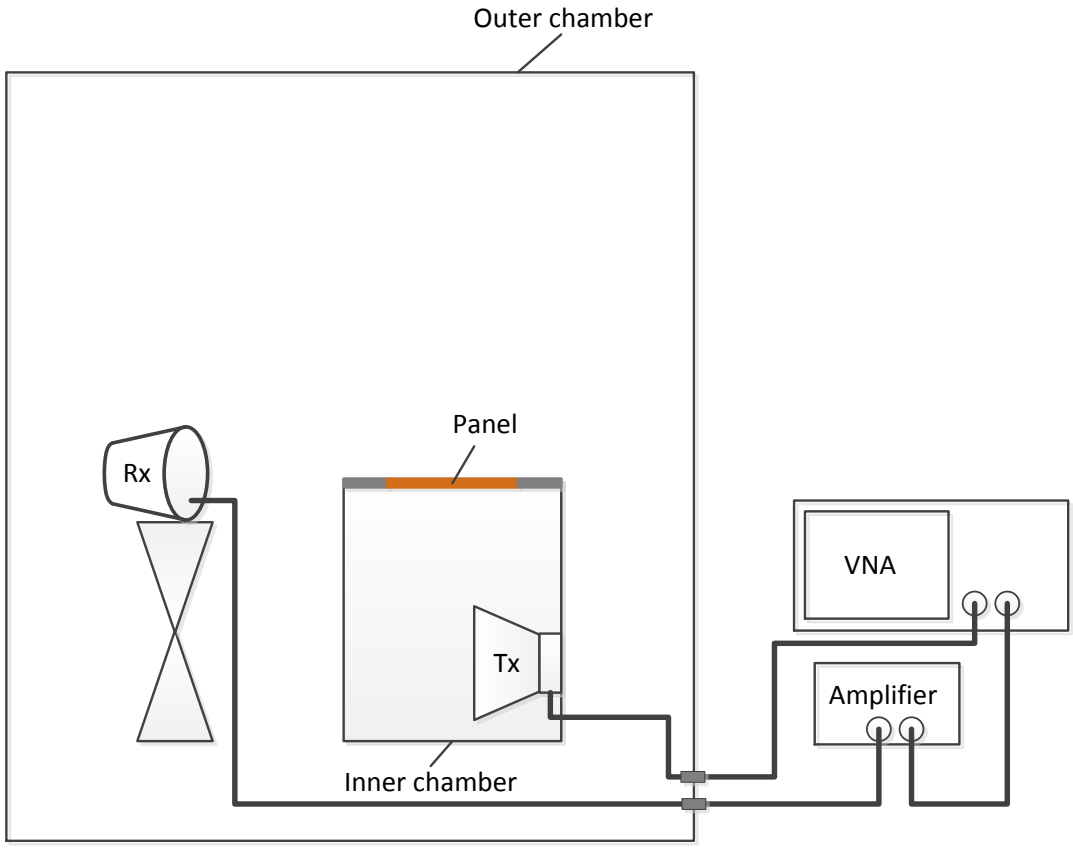

Figure 2.24 SE measurement setup for waveguide panel

There is one horn antenna in the small enclosure as a transmitting antenna (Tx) (Figure 2.26), and another V-type log-periodic antenna is placed outside the small enclosure but still in the shielded tent as a received antenna (Rx) (Figure 2.25). The Tx antenna is excited by the output of the network analyzer (VNA) and then the signal will go out from the small enclosure to be received by the Rx antenna. The input port of the network analyzer will catch the signal from the received antenna via a preamplifier.

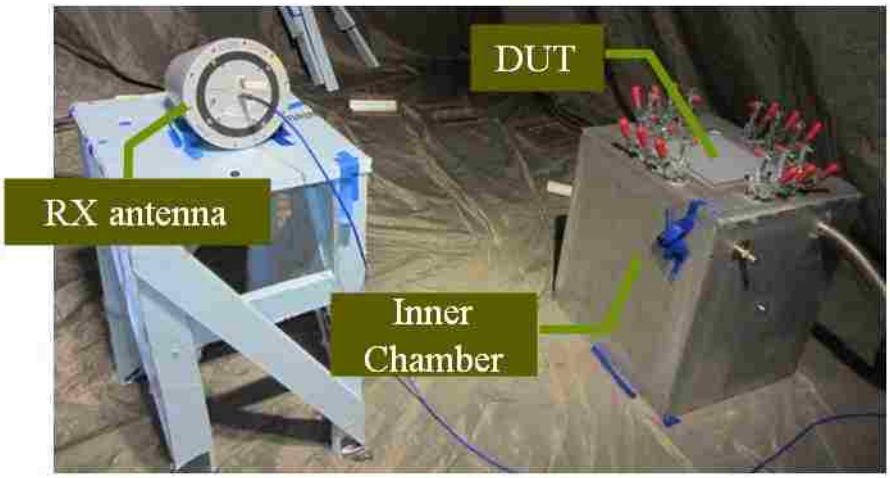

Figure 2.25 SE test vehicle in the tent

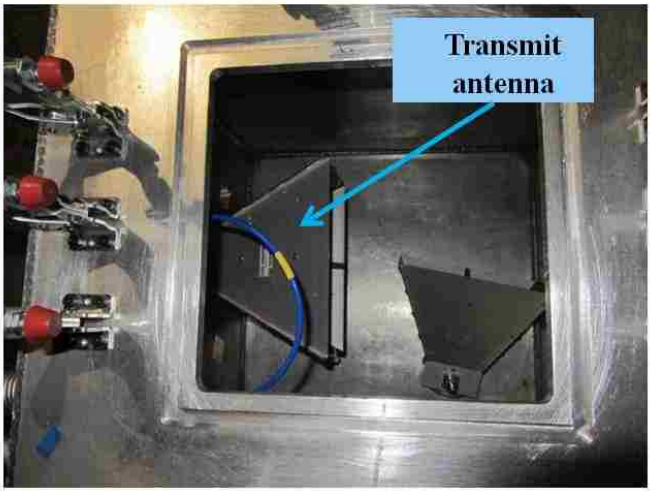

Figure 2.26 Transmit antenna in the small enclosure

The S_{21} is measured by the network analyzer in the cases of with or without a waveguide panel sample installed on the top of small enclosure. Moreover, for the whole testing, there is no change in any other setup, such as antenna positions, small enclosure position, cable positions, or VNA setting. Therefore, the SE of the waveguide panel could be defined as Eq. (19).

$$SE_{dB} = S_{21\ dB\ without\ panel} - S_{21\ dB\ with\ panel} \tag{19}$$

$$\langle |S_{21}|^2 \rangle = \frac{1}{N}\sum_{i=1}^{N}|S_{21}(f_i)|^2 \tag{20}$$

Where

$$N = \frac{BW}{\Delta f} + 1 \tag{21}$$

Where BW is the bandwidth used in this frequency averaging (or frequency stirring) approach and Δf is the width of the frequency step used in obtaining the data. This averaging process requires taking the magnitude squared of the complex-valued S parameter for a given frequency then summing over the frequencies in a given BW. N is given by Eq. (21).

In determining the shielding effectiveness as Eq. (19), ensemble averages for both S21 as Eq. (20) of with and without panel on the small chamber. Details on the calculation and MatLab codes are attached in the Appendix.

The network analyzer setup could be as shown in (Table 2.3). To obtain a good dynamic range for the SE measurement, the maximum output level of VNA and lower IFBW value should be used.

Table 2.3 VNA setting for SE measurement

Network Analyzer Setting	
Frequency	1GHz to 20GHz
IFBW	100Hz
Sweep points number	6401
Output level	10dBm

The waveguide panel sample will be fixed in the aperture of a small enclosure. Actually, the panel samples will slightly smaller than aperture to allow us to carry out some treatments for the edge of panel. The contact between the panel edge and the inner surfaces of the aperture is very important. A poor contact will cause strong EM leakage, which is too strong to identify the real performance of the panel itself. After undertaking measurements, we select fine copper wool as the gasket material, as it is soft and very conductive to reducing the leakage from the panel edges (Figure 2.27) (Figure 2.28).

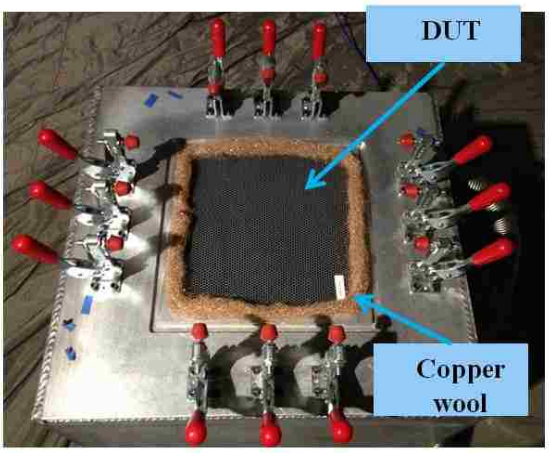

Figure 2.27 Waveguide panel installed on the small enclosure

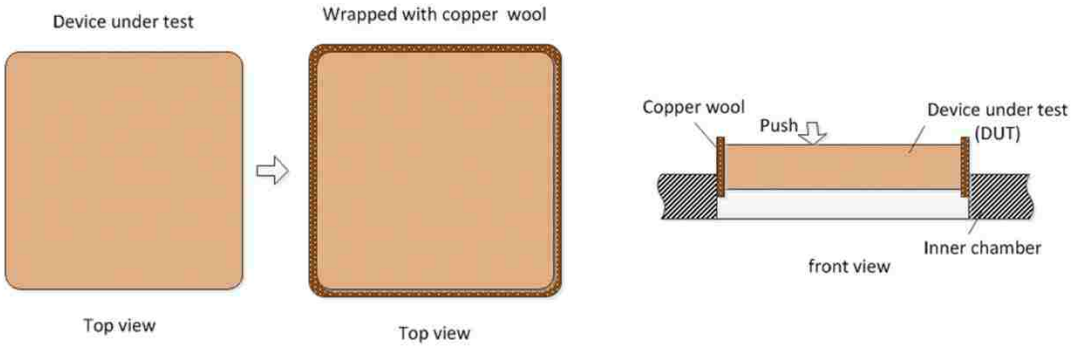

Figure 2.28 Installation procedure of waveguide panel

As the reference, (Table 2.4) lists all equipment used in the measurement. Since the SE measurement is a relative measurement, the results are repeatable and stable if the setup does not change in both with and without panel cases.

Table 2.4 Equipment list for SE measurement

Equipment list	
Tx antenna	ETS 3115 horn antenna (0.8GHz to 18GHz)
Rx antenna	R&S HL050 V-log-periodic antenna (0.5GHz to 20GHz)
Shielded tent	MS&T EMC LAB, conductive fabric, 4m x 4m x 3m
Network analyzer	Agilent PNA-X (10MHz to 50GHz)
Pre-Amplifier	HP 8449B (1GHz to 26.5GHz)
Cables	SMA connector, x 3, (DC to 26.5GHz)
Small enclosure	MS&T EMC LAB, aluminum, 0.8m x 0.8m x 0.8m

2.3.3. Dynamic Range of Measurement System. Before the measurement for the waveguide panel, the dynamic range of whole measurement system should be measured, which shows the maximum shielding effectiveness can be measured by current setup and configuration.

The dynamic range is determined by the shielding effectiveness when the opening on the small chamber was totally sealed by blind metal panel; therefore, there is only the noise floor of system.

Figure 2.29 Open top of small chamber

Figure 2.30 Sealed top of small chamber by blind panel

Firstly, measure the $S_{21\text{-open}}$ when the top of small chamber opening, which as the reference for SE measurement (Figure 2.29). And then, clamped a blind metal panel tightly on the top opening of small chamber (Figure 2.30), for the best sealing, also use some copper wool beneath the panel to make better conductive contact with chamber, and obtained the $S_{21\text{-seal}}$.

After the ensemble average for S-parameters by Eq. (20), in dB scale, the dynamic range of system is given by Eq. (22).

$$SE_{dynamic-dB} = S_{21\ dB\ open} - S_{21\ dB\ seal} \quad (22)$$

The dynamic range is the upper limit of system for the SE measurement, in other word, if the SE performance of one waveguide sample is higher than this dynamic range, its exact number won't be known. By the Eq. (22), increasing the input power or decreasing the IFBW of network analyzer could help higher the $S_{21\text{-open}}$ or lower the $S_{21\text{-seal}}$, thus get a larger dynamic range.

The dynamic range is repeatable and stable for a certain measurement setup, any changing in measurement configuration such as antenna position, instruments setting or cable type will get a different dynamic range. Therefore, the dynamic range and SE measurement of waveguides must be performed at the both exact same setup and same time. (Figure 2.31) show the dynamic range of current measurement setup.

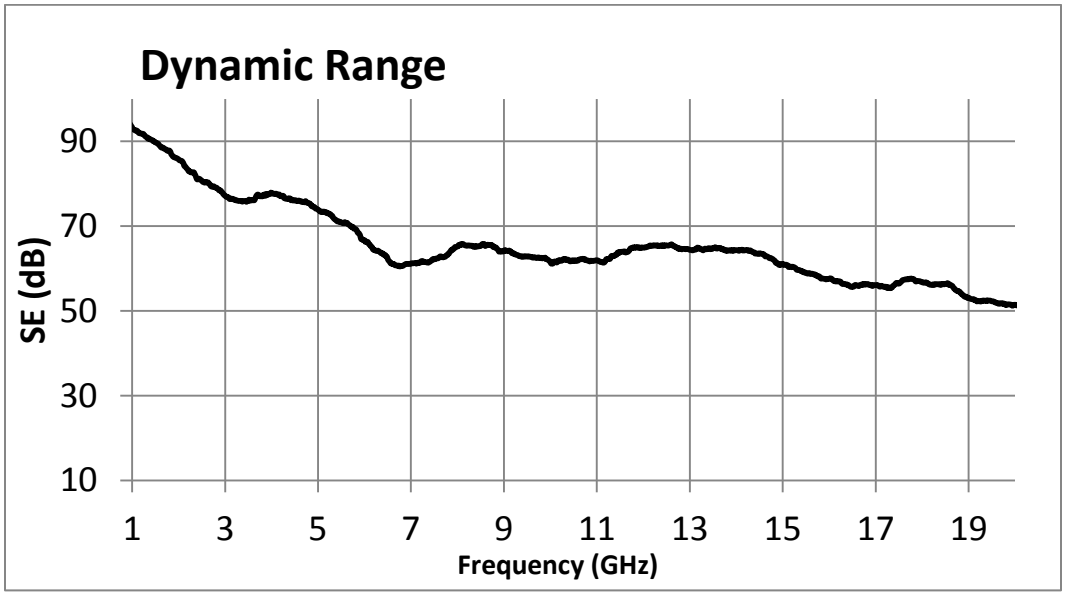

Figure 2.31 Dynamic range of measurement system

In terms of above plot, the SE measured by current setup can't over that value.

2.3.4. Measurement Results. According to the above measurement methods and setup, we select six waveguide samples for the SE measurement. One of them is made of pure aluminum, a traditional waveguide panel, as reference. (Table 2.5), shows the basic parameters of samples.

Table 2.5 Sample list

Sample #	Core material	Coating material	Panel thickness (inch)
1	Aluminum	/	0.5
2	Polyetherimide (PEI)	Al 0.4 μm	0.5
3	Polyetherimide (PEI)	Al 0.6 μm	0.5
4	Polyetherimide (PEI)	Al 2 μm	0.5
5	Polyetherimide (PEI)	Al 4 μm	0.5
6	Polyetherimide (PEI)	Al 0.2 μm	0.25
7	Polyetherimide (PEI)	Al 2 μm	0.25

As mentioned before, the panel edges are sealed by fine copper wool during the entire measurement, so the results reflect the SE performance of the sample itself. (Figure 2.32) to (Figure 2.38) show the SE results for all samples. For the comparison, all the results for MaxAir samples shown with the dynamic range and result of aluminum panel (sample 1). Since the panel is a plastic-based material, which is soft and easy to break, very careful attention when installing it on the cavity with copper wool must be paid, but it still induces an uncertainty for each time measurement. In our measurement, we measure each sample twice, do the complete reinstallation each time, and select the best results from them.

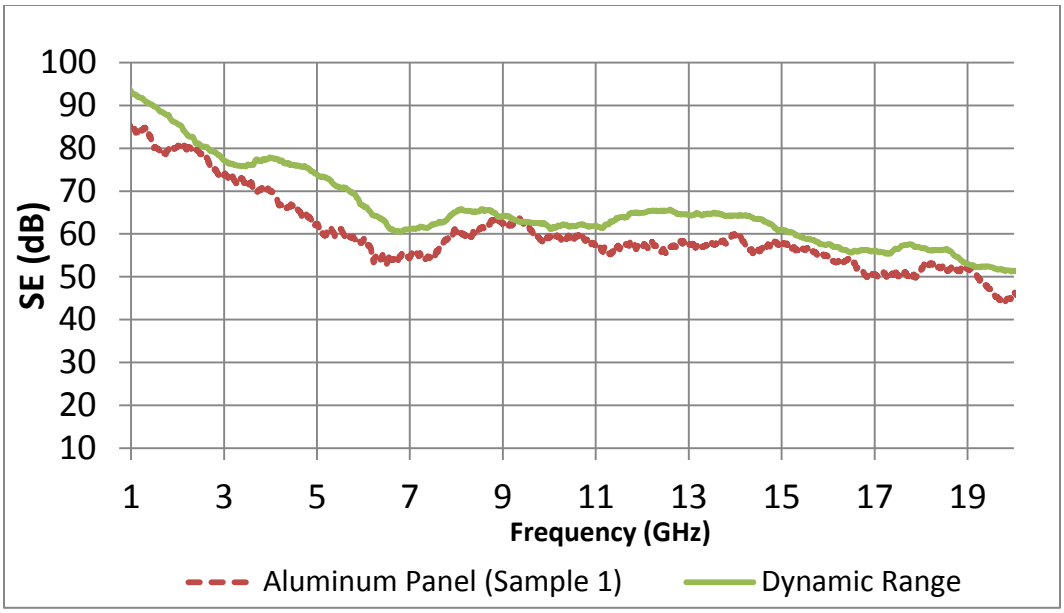

Figure 2.32 SE result of sample 1

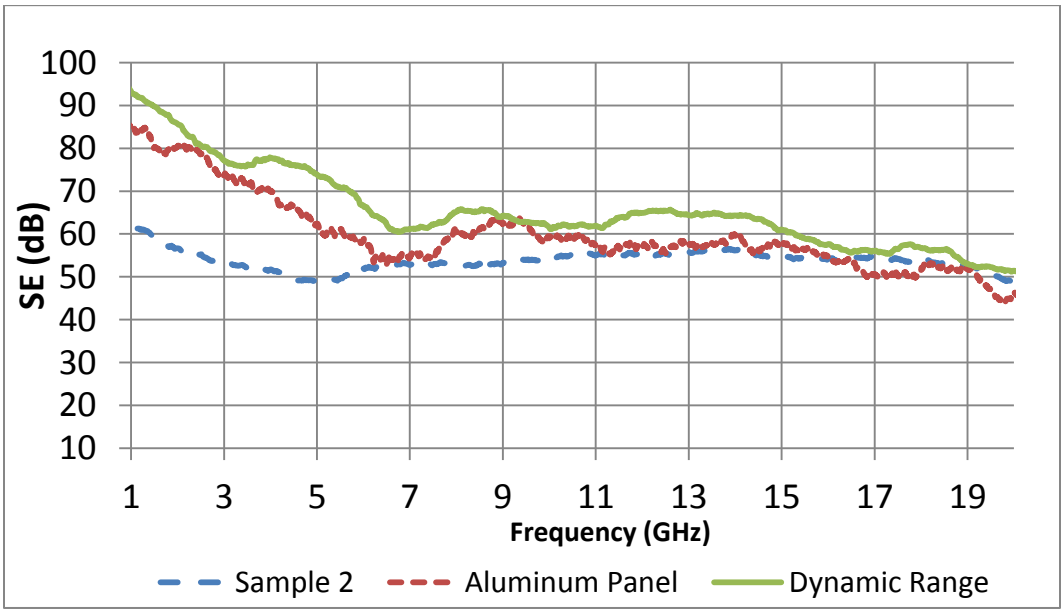

Figure 2.33 SE result of sample 2

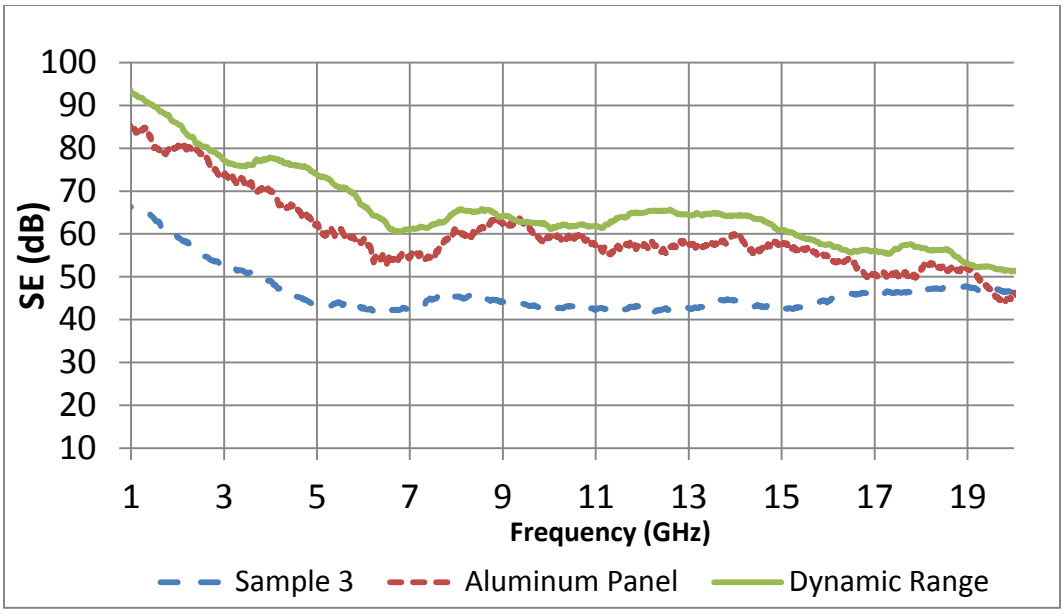

Figure 2.34 SE result of sample 3

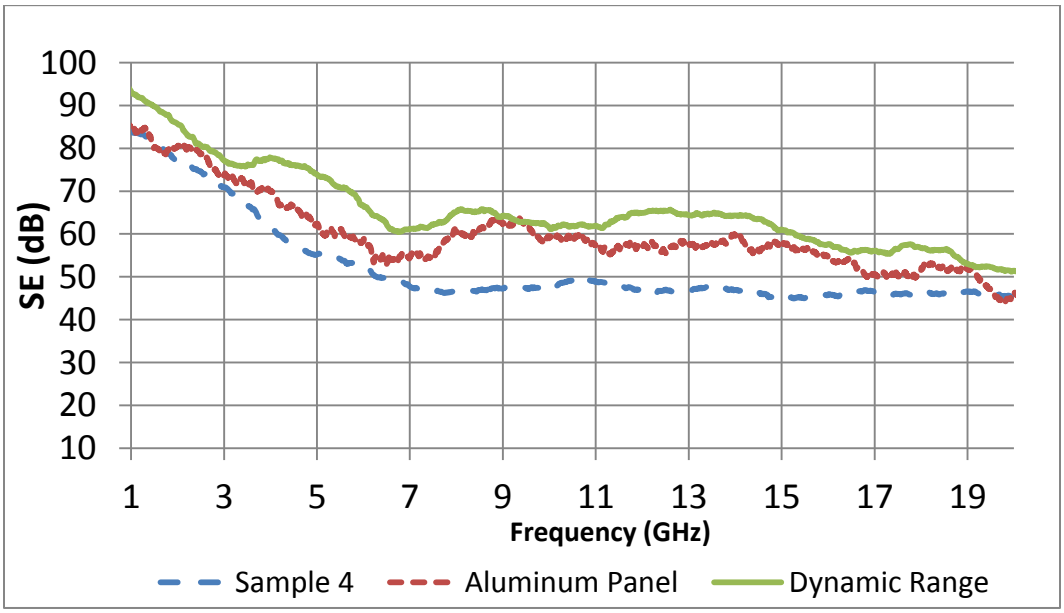

Figure 2.35 SE result of sample 4

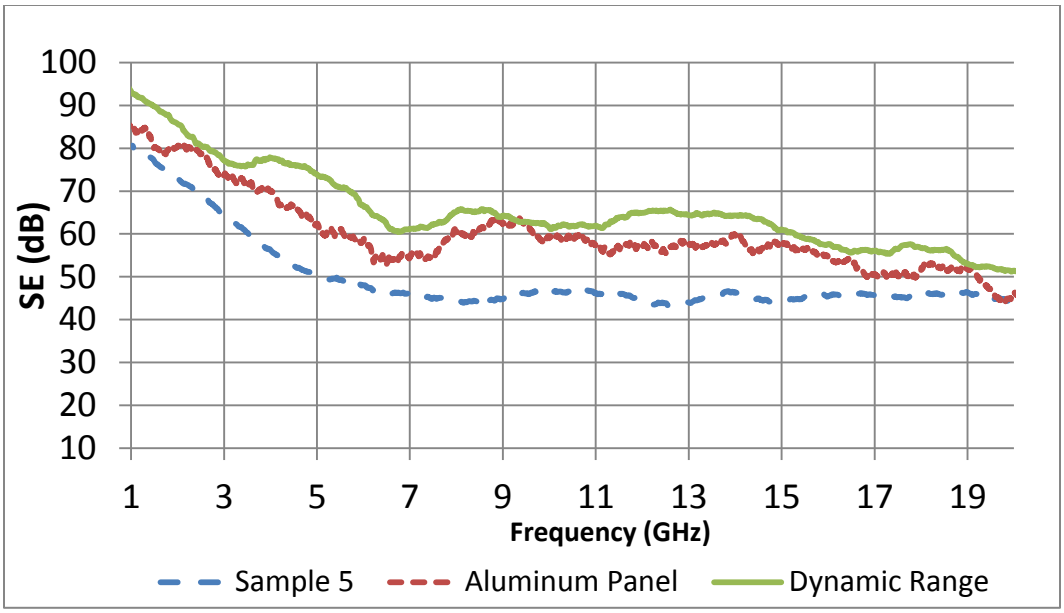

Figure 2.36 SE result of sample 5

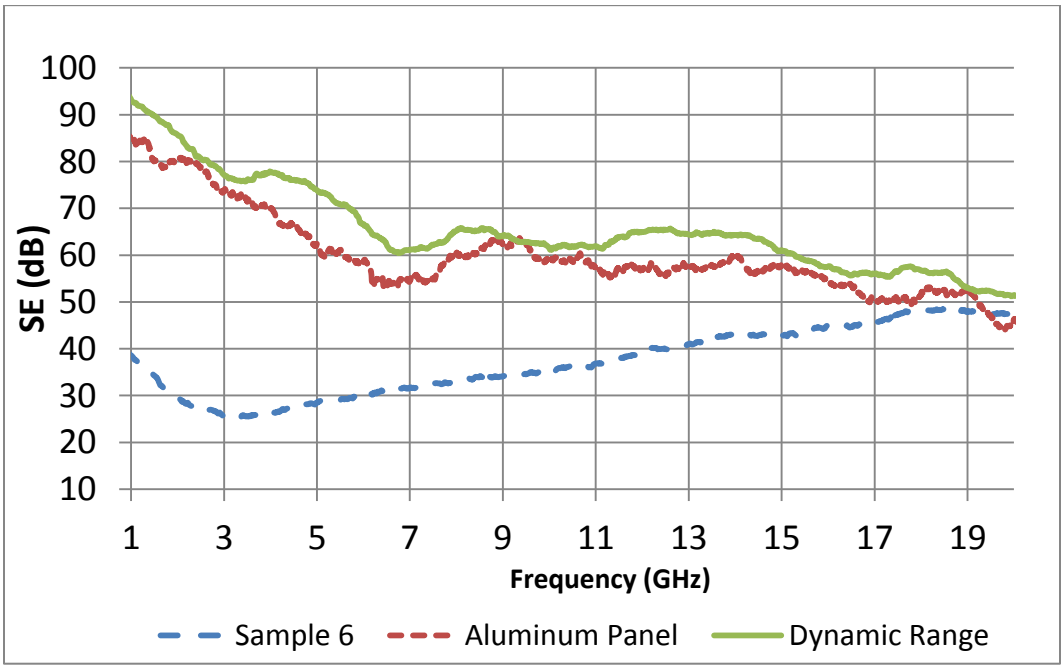

Figure 2.37 SE result of sample 6

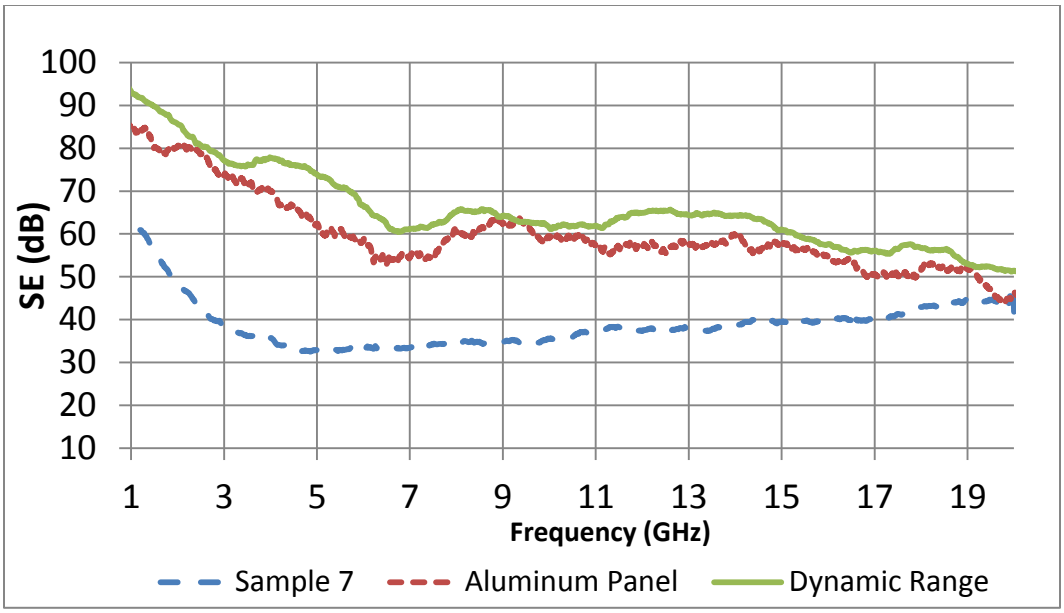

Figure 2.38 SE results of sample 7

2.4 RESULTS ANALYTSIS

From the SE results above, Sample 1, the traditional material, gives the best performance from 85–45 dB in 1–20 GHz. It should be better than that in terms of the simulated result. The test vehicle does not have enough dynamic range at higher frequencies since the signal will attenuate rapidly with path distance, even if we use a preamplifier. Therefore, Sample 1 hit the limit of dynamic range.

For Samples 2–4, with the increase in metal coating thickness, the SE of the plastic core based panel kept going up at lower frequencies. However, the SE of Sample 5 shows no change, even though its coating is thicker than Sample 4. This means the SE will not be effected when the coating thickness more than its skin depth. Therefore, ensuring the proper amount of coating helps with the SE issue.

Compared with Samples 1 to 5, the thickness of Samples 6 and 7 changes to 0.25 inches. This significantly worsens the SE, but the coating thickness still affects the SE by the same tendency. The half thickness panel also has a smaller contact area with the copper wool, which could cause more leakage from the panel edges.

In terms of the SE results of the seven samples, we know that the SE performance

of the metal-coated panel will be affected by the coating thickness when the coating thickness is near the metal skin depth. With the proper coating, though the coated panel is not as good as the traditional one, considering its lower cost, it is good enough for some low-level requirements.

In our measurements, soft copper wool is used for edge sealing, but it is not the solution for the real application. The plastic-based panel is too soft to be treated as traditional one. For future studies, it is important to find the most effective and practicable edge treatment for coated panels.

3 MATERIAL EVALUATION BY LAPTOP APPLICATION

3.1 INTRODUCTION OF LOSSY MATERIAL APPLICATION

EMI (Electromagnetic Interference) has become a major issue in the field of electronics in the last few years, with higher and higher frequencies being used. The noise from EMI not only affects devices outside the source device, but it also affects the device itself. This affection turns more obvious with the higher frequency and lower power of current electrical technology.

A design of wideband nonconductive absorbing shielding enclosures, protecting screens, wallpaper, coatings with specific filtering properties, and gaskets is important for solving numerous problems of electromagnetic compatibility (EMC) and improving immunity of electronic equipment. Composite EM wave absorbers and noise-suppressor sheets protect susceptible devices, components, and circuits by absorbing undesirable radiation, by eliminating possible surface currents and cavity resonances, and by diverting or terminating unwanted coupling paths. Combining dielectric or conducting inclusions with ferrite or magnetic alloy inclusions in a composite may increase the absorption level substantially in the frequency range of interest The latest laptop computers have faster CPUs and memory. They communicate with each other through high-speed buses. These are all powerful potential noise sources. Mutual interference may reduce their performance [12].

It is important that when applied to electronic products, the engineered absorbing materials would allow for analysis EMC, electromagnetic immunity, signal integrity (SI), and power integrity (PI) over the frequency ranges of interest. For applications in high-speed digital electronic designs, the materials that would absorb EM energy in RF, microwave, and potentially mm-wave bands, are of special interest. Thin absorbing noise-suppressing composite sheets and coats are of special interest for such applications, especially because of microminiaturization trends and for the convenience of applying directly on the surfaces to be protected and their broadband performance. Thin sheet absorbers can wrap cables, be applied directly on the sources of noise, or at some optimal distance from the source. They can be put directly on the electronic module enclosure, around or over vents, holes, sharp edges, and wedges, or may be placed as patches inside cavities to damp unwanted resonances [13].

To eliminate EMI, using a lossy absorbing material (Figure 3.1) on the main noise source is an effective method, in addition to shielding. By applying these two methods, we can use them alternatively to evaluate absorber material performance. There are many kinds of absorbing material for selection. The most popular one for computer or portable device application is a cavity absorbing material, which used for resonance application, and the parameters of the material include high magnetic and/or dielectric loss over a broad range of frequencies. If the material could be place on right place, it would solve the EMI problem for the device.

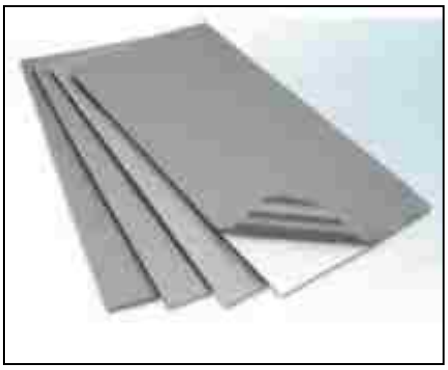

Figure 3.1 Lossy absorbing material

3.2 TYPICAL EVALUATION METHOD FOR ABSORBING MATERIAL

The entire procedure of absorbing material development consists of a chemical property study, an EM parameter simulation, and material evaluation. Besides the modeling and numerical analysis, high accurate evaluation methods play an important role in material development and could help in finding the real parameters of the material to validate the simulated results further. The application of materials depends on the effective frequency of the material and in terms of accurate, evaluated results.

A current objective is to develop a methodology to design and evaluate novel products efficiently based on absorbing magneto-dielectric composite materials primarily for EMC/EMI purposes [13]. (Figure 3.2) shows the engineering design of noise-

suppressing materials and EM filtering structures [13].

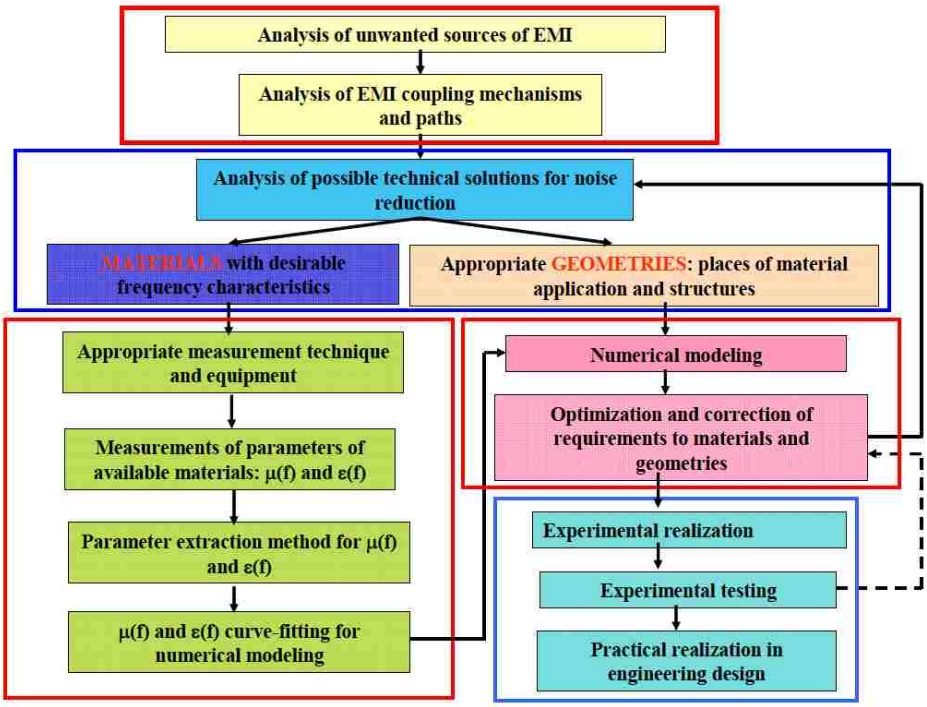

Figure 3.2 Flowchart for engineering design of EMI noise-suppressing materials and structures

The typical evaluation method of material includes two parts: the parameter measurement of the absorbing material by the airline method, which can tell both the accurate permittivity and permeability of the tested material, and validation measurement by the micro-strip test board. With that, we obtain repeatable results to compare with the simulated ones for the validation of material parameters.

The experimental setup (Figure 3.3) was used to measure the material parameters of the samples of the absorbing materials. The test samples are shaped as washers with the dimensions to fit the cross-section of the standard 50-Ohm 7/3-mm coaxial airline, which is used as a sample holder. After the TRL (“through-reflect-line”) calibration that

removes port effects in the frequency range of interest, the S-parameters on the test line are measured. Then the relative permeability and permittivity are extracted using the standard Nicolson–Ross–Weir (NRW) procedure [14].

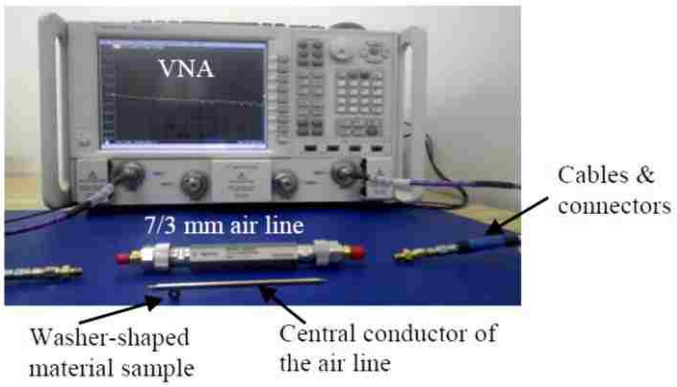

Figure 3.3 7mm Air-Line method setup

The validation measurement using micro-strip line test board for absorbing materials is relatively simple compared with the airline method. Tightly putting a particular size of material sample in the certain position of a single-ended micro-strip line could change the single-ended S-parameter. The difference in the S-parameter with or without material on the line indicates the influence from the material. Since the structure of the micro-strip is so simple, obtaining repeatable measurement results and good agreement with simulated ones is straightforward.

For the whole measurement setup (Figure 3.4), the test board has a single-ended micro-strip line of width 3 mm (50 ohm in the 62-mil thick PCB), then the two ports' S-parameters are measured using the network analyzer. During the measurement, the material should be clamped by a piece of foam to contact the trace tightly.

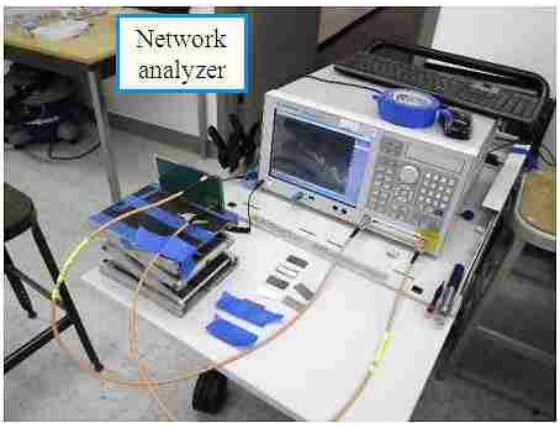

Figure 3.4 Material validation method setup based on micro-strip

3.3 POSSIBLE NOISE SOURCE IN THE LAPTOP COMPUTER

Before applying the material to a real application, the relative parameters of the application should be known first, including EMI frequency range, type of EMI (electric or magnetic source), and emission level of EMI. Then, a suitable material for this application based on these parameters should be chosen. First, the material performance needs to be evaluation. There are several methods, such as airline measurement and waveguide measurement, to test the performance of an absorbing material. For a specific application, the evaluation method based on real application will more intuitive.

The laptop noise reduction is a typical application for cavity absorbing material. By using a laptop, we can develop measurement methods to evaluate absorber performance.

Most of the current laptop computers are composed of basic components, such as display, hard disk, memory, wireless module, and motherboard. Each of them will generate EM noise, and some work at several Gb/s data rate with increasing computer processor speed. The higher the data rate, the higher its clock frequency.

The mainstream wireless technology, like 802.11n or Bluetooth, uses the 2.4–2.5 GHz frequency band (Figure 3.5). This frequency band will cause EM noise from inner components of a computer, which in turn may cause interference.

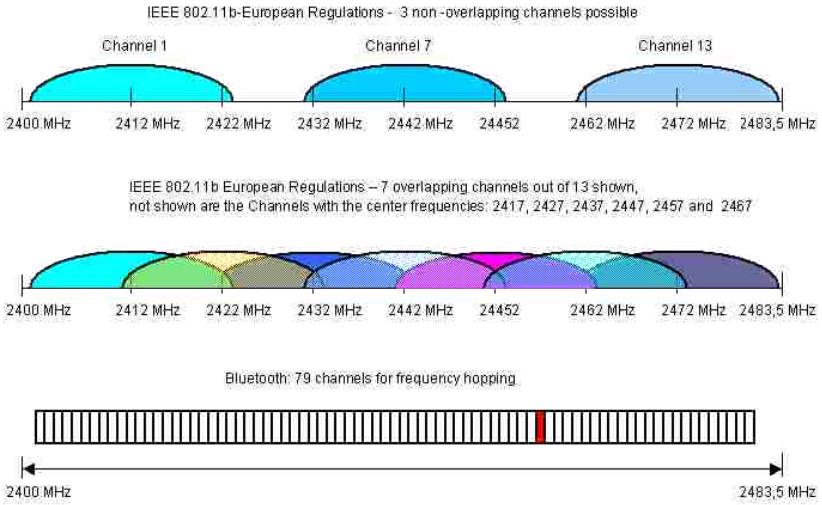

Figure 3.5 Bandwidth for different wireless technology

The volume budgeted for Wi-Fi/Bluetooth antenna integration can often approach or attempt to violate the fundamental bandwidth and gain the limits of electrically small antennas [15]. This can lead to high sensitivity for the narrow-band noise, around 2.4 GHz. Such noise may have a significant impact on the performance of the other narrow-band systems, such as those based on IEEE 802.11a/b, which operate at 5–6 and 2.4–2.48 GHz, respectively. As a typical scenario, consider a computer that uses IEEE 802.11 to ensure LAN and Internet connection and a video card processing high data rate video stream and memory cards [16].

The computer processor and hard disk are usually well shielded. One of the main noise sources is the memory. Currently, the newest memory is DDR4; its clock speed can go up to 2.4 GHz. The memory card has been designed as a removable part, so it is convenient for a noise study.

Unintentional noise between the ground-reference plane of a daughter card (such as a memory module) and the ground-reference plane of a motherboard can cause significant emissions within a system. These emissions are due directly to the EM1 ‘noise’ across the memory card connector. The source of this ground-to-ground noise is the intentional currents that are driven on the memory bus [17].

The antenna is the most sensitive part in a laptop wireless system. It is sensitive to

signals and noise, and the noise-coupling path is shown in (Figure 3.6 Therefore, we can use the laptop's built-in antenna to measure noise from the memory. The position of the built-in antennas in laptops will vary; they are used for Wi-Fi or Bluetooth and are usually placed in the lid (screen cover). (Figure 3.7) (Figure 3.8) show examples of a typical laptop, its antenna position on the screen cover, and a memory card. In terms of noise coupling mechanism in laptop, we designed two measurement methods for material evaluation: noise floor measurement and data rate measurement.

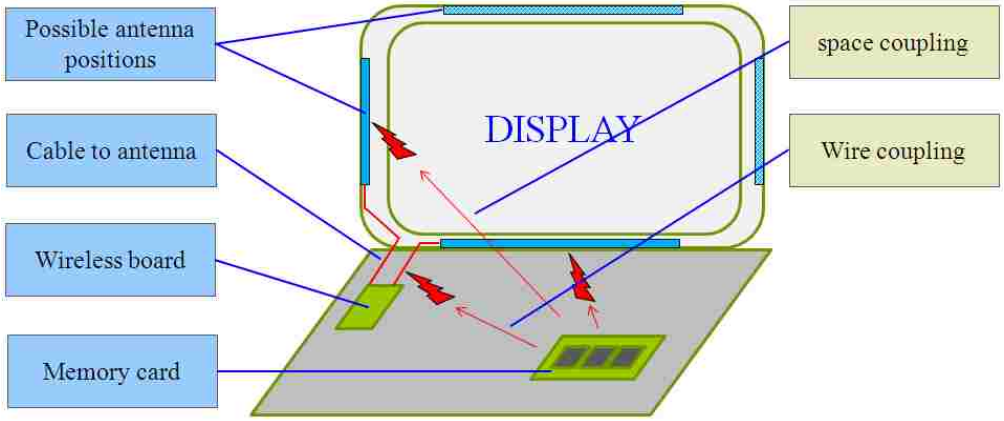

Figure 3.6 Noise coupling paths inside the laptop

Figure 3.7 Example of laptop

Figure 3.8 Example of inner structure of laptop

In terms of the coupling mechanism by inner parts of laptop, we evaluate mainly the influence of absorbing material by two measurement methods. The first one measures the EM noise around 2.4 GHz via the Wi-Fi/ Bluetooth antenna inside the laptop to see what the noise from the inner components of laptop looks like. Then, we re-measure after putting the lossy absorbing material on the memory socket pins. The difference between two cases is the influence from the protecting material.

In the second method, we build a Wi-Fi communication between the two laptops and record the data rate at different transmitting levels in the case with or without the laptop fully running. When the laptop is in the fully running condition, more EM noise from inside of computer will worsen the Wi-Fi performance. Then we also put lossy material on the memory socket pins to see how the Wi-Fi data rate changes. Thus, we evaluate the property of the absorbing material.

3.4 LAPTOP NOISE FLOOR MEASUREMENT METHOD

In the laptop computer, noise from the memory (the aggressor) can be transmitted to a built-in antenna (victim) through various ways: wire coupling or radiation through vents. Due to that, the noise floor of the Wi-Fi system will increase. When placing an absorbing material in a certain position on the memory, the memory chip’s noise emissions will be reduced.

The laptop’s build-in antenna can detect this kind of reduction, so measuring the various memory noise levels using the built-in antenna of a laptop, both with and without absorbing materials, will quantify the improvement of an absorbing material.

3.4.1. Measurement Setup. The equipment set-up to measure the noise in the computer by the built-in antenna includes a laptop, spectrum analyzer, and low noise preamplifier (Figure 3.9). Both the spectrum analyzer and preamplifier should work in the 2.0–2.5 GHz (the Wi-Fi and Bluetooth worked at 2.4 GHz). The level of memory noise is low, even if the memory is being fully accessed. A preamplifier is used to amplify the signal but will also affect the wireless communication. The use of a spectrum analyzer moves the signal through the preamplifier from the built-in antenna. The setup shown in (Figure 3.9 is placed in a shielded room, which will isolate the EM noise from the outside environment, as shown in (Figure 3.10).

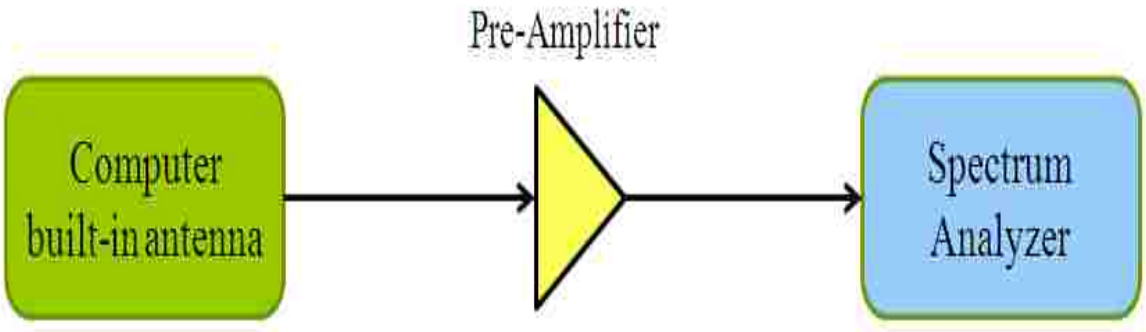

Figure 3.9 Noise floor measurement setup diagram

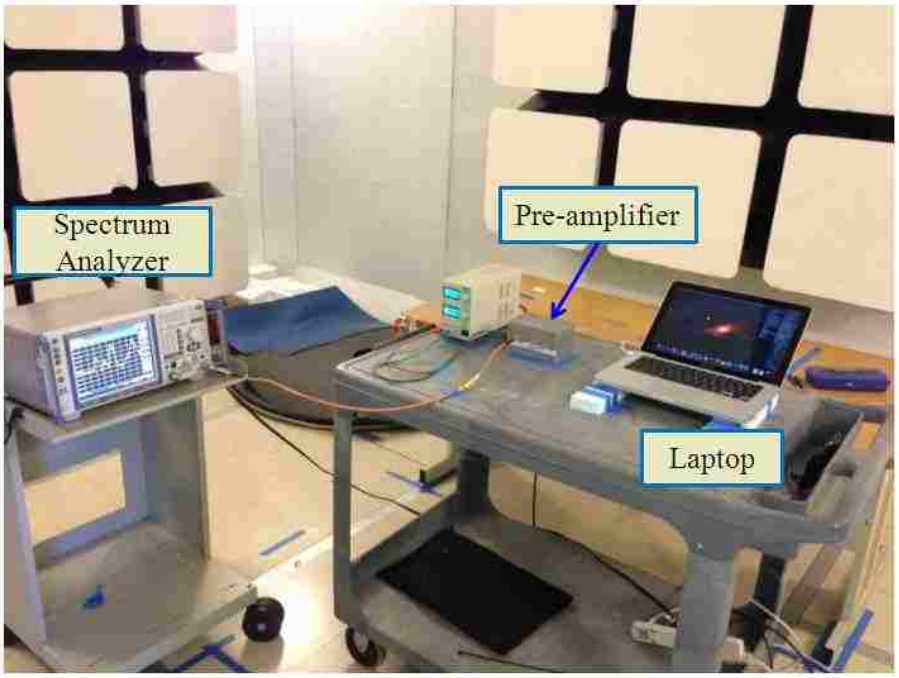

Figure 3.10 Measurement setup in shielded room

The test computer has two antennas below the display, which are hidden by the display panel, as shown in (Figure 3.11). The blue circle marks the position of the build-in antenna. We used one of them as the receiving antenna to connect to the preamplifier.

Figure 3.11 Connect the pre-amplifier to built-in antenna

Since the antenna connector is a press-in connector, it is small and not tight enough, so we used conductive fabric to cover the connections to reduce interference and measurement instability (Figure 3.12).

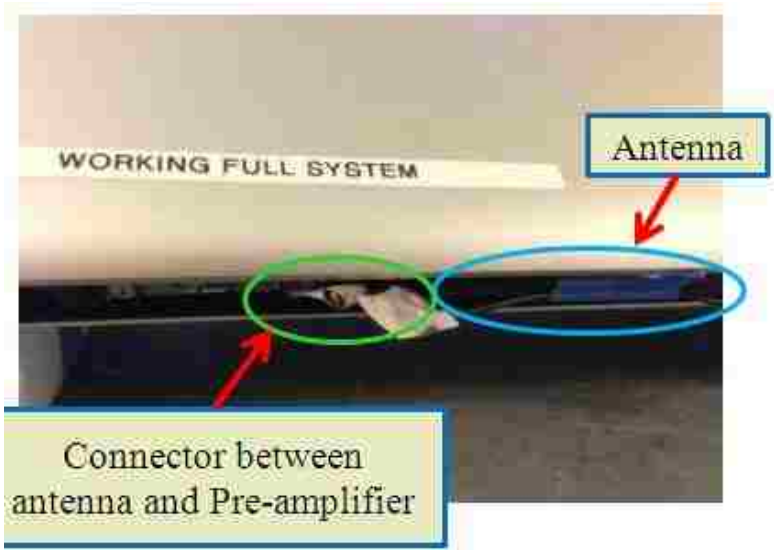

Figure 3.12 Treatment of the antenna connector

The entire measurement was performed for two cases: with and without material. This enabled us to measure the material performance. Through the near field scan, the strong noise source around the memory is located in the memory pins, which connect the memory to the motherboard. As its dimension is suitable for EM radiation, we cut the absorbing material to 7 cm × 1.5 cm to fit over the memory pins (Figure 3.13).

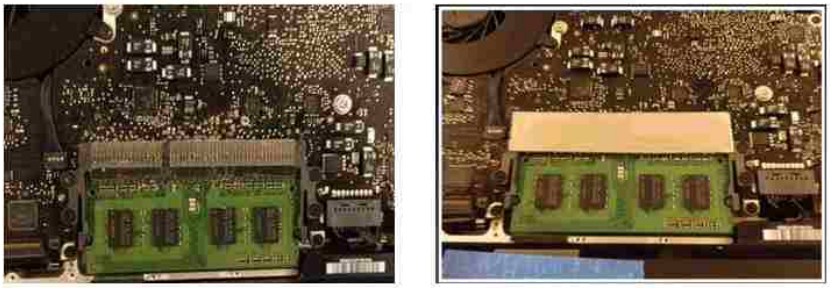

Figure 3.13 Material location in the laptop

Evaluating the material performance requires the laptop to work in a certain status to obtain maximum noise from the memory. There are three defined cases of the laptop computer for results comparison.

a) ‘Idle’ case: Close the applications as much as possible in the laptop except OS, so there is less access to the memory card. From this, we get the smallest memory noise as a reference line.
b) ‘Busy’ case (vertex case): Run testing software called ‘Vertex Performance Test’, which forces the laptop to do a heavy calculation with continuous access of the memory card. This case gives the largest noise from the memory.
c) ‘Absorber Material’ case: The laptop is run as in the ‘Busy’ case, but with a test piece of absorber material on the pins of the memory card.

All the instruments used in the measurements are shown in (Table 3.1).

Table 3.1 Instruments list for noise floor method

Instrument Name	Model	Comment/Setting
Computer	13 inch display	Use one of the antennas to receive memory noise, could run in both ‘Idle’ and ‘vertex’ cases.
Spectrum analyzer	R&S FSV	Frequency:2.35 GHz to 2.5 GHz Sweep points: 1000 Internal ATT: 5 dB BW: 10 kHz Sweep time:100 ms Ref level: -30 dBm
Power limiter	Agilent N9356C	/
Pre-amplifier	/	Gain: 40 dB
Cable	SMA 0.5 m	Install by torque wrench.

3.4.2. Measurement Steps. The measurement steps are as follows:

1) Prepare the measurement setup per Figure 3.7. Set all instruments with the parameters as Table 1, then perform the measurement as follows.
2) Position the laptop display panel at max angle in every measurement.
3) Warm up system for 0.5 h to stabilize the computer and preamplifier.
4) Close all software on the computer except OS; turn off any other wireless devices.
5) Make sure there is no absorber material in the computer.
6) Tighten all screws. Keep display brightness at 50%, then record the signal level by ‘Maxhold’ of the spectrum analyzer, and keep 1 min for every measurement. Measure three times and record the data; use three times the average data as the result.
7) Run the ‘vertex’ tool, then repeat steps (4) and (5)
8) Open the back cover of the laptop and place the test piece of absorber material on the memory pins. Run ‘vertex’, and repeat step (5) to obtain the material measurement results.
9) After all materials are measured, repeat steps (3) to (6) to check the repeatability of the system and verify no drift occurred.

3.4.3. Measurement Results and Discussion. By measuring, we can define the noise floor for the three different material cases. The amplitude unit of noise is dBm. We select the results of one material sample as an example; see the results in (Figure 3.14).

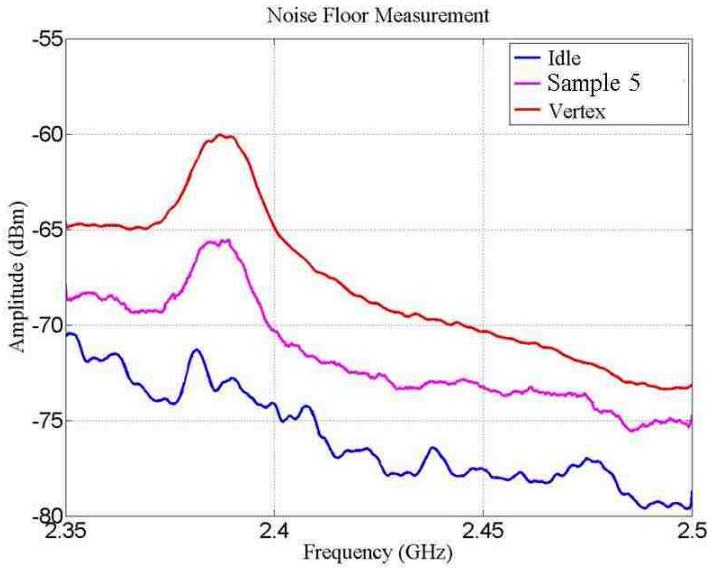

Figure 3.14 Noise floor results (example)

The red line shows the noise level measured in the condition of 1) the laptop fully running and 2) without absorbing material. The noise is high, so we got the highest amplitude value. When we change the laptop operating mode to the 'idle' case, there is no software running in the laptop except OS, in other words, the memory behaves as 'doesn't work', so the blue line gave the lowest level. When the absorbing material has been added, as the pink line shows, the difference between the 'Vertex' and 'Idle' proved this material could reduce the noise. The difference between 'Vertex' and 'Material' noise enables us to directly evaluate the performance of material, see (Figure 3.15).

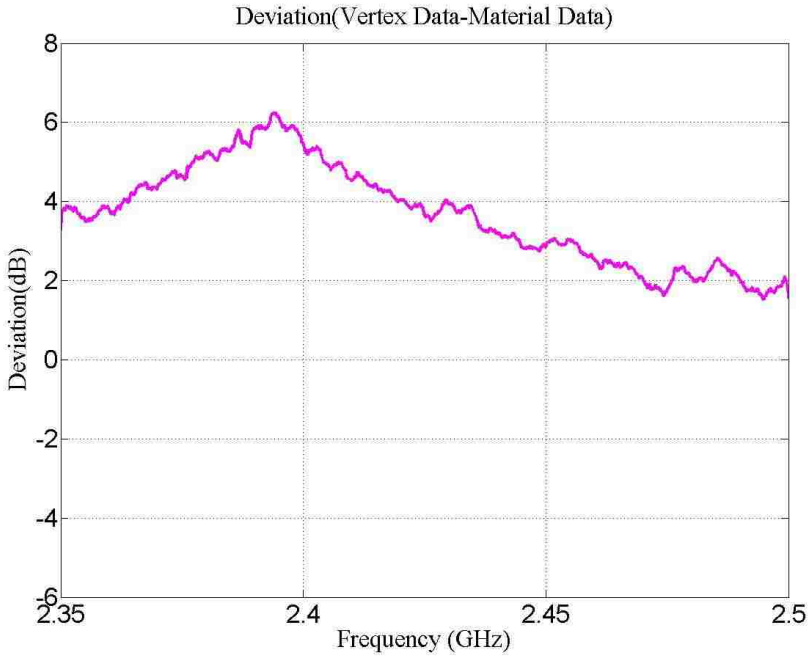

Figure 3.15 Deviation of noise floor (example)

3.5 WI-FI COMMUNICATION MEASUREMENT METHOD

The noise from the memory card of the laptop will affect wireless communication by direct antenna coupling and indirect relevant circuit coupling. For these types of interference, the most obvious performance decay of wireless communication is the transfer data rate reduction. Base on this phenomenon, we could build a wireless connection between two computers to measure the data rate with the decreasing signal output power, until to the data rate is 0 or the connection fails. Due to the memory noise, the minimal signal level that could keep Wi-Fi connection will be larger than without memory noise case. In terms of this kind of relation of signal level and data rate, we can find out how specific absorbing materials could improve the wireless communication.

3.5.1. Measurement Setup. To build a Wi-Fi data transfer before the measurement, we need to use two laptops to build a Wi-Fi communication: one is the ‘server’ computer, the other one is the ‘client’ computer (Figure 3.16). To avoid other ‘noise’ from the Wi-Fi signal interference in the air, we need to put the ‘server’ in the shielded anechoic chamber (Figure 3.17), and let the Wi-Fi signal of the ‘client’ go into

the chamber via a 2.4 GHz monopole antenna (Figure 3.17) (Figure 3.18), This way, both wireless signals of the two laptops will stay in the chamber, and any outside ‘noise’ will not affect the communication.

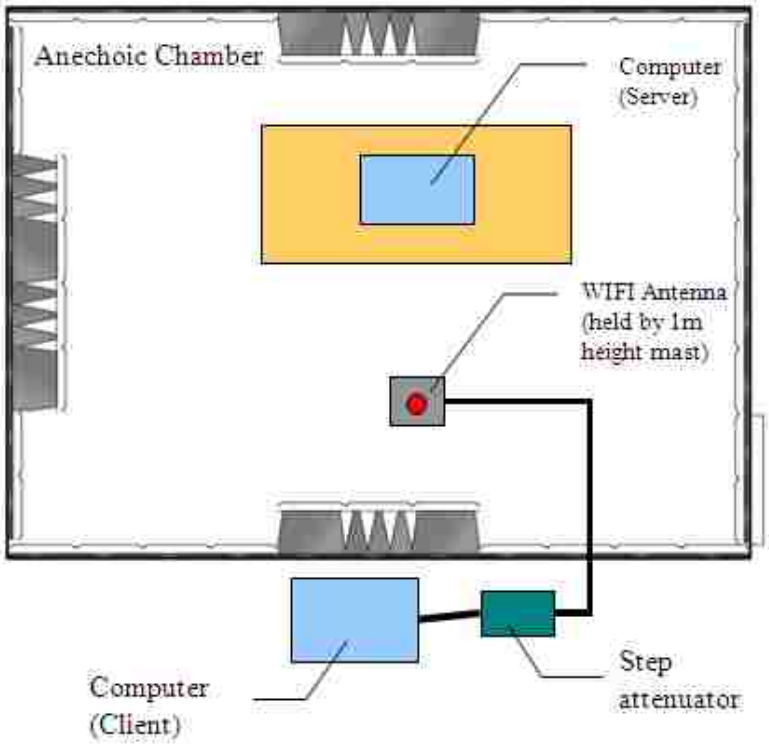

Figure 3.16 Setup of Wi-Fi communication measurement

Since it is hard to control the Wi-Fi signal level in the computer, a special wireless driver from manufacturer may be required, so we use a step attenuator to decrease the signal level (RSSI, Received Signal Strength Indicator), and measure the data rate using the ‘server’ laptop (Figure 3.17).

Figure 3.17 Setup inside the chamber

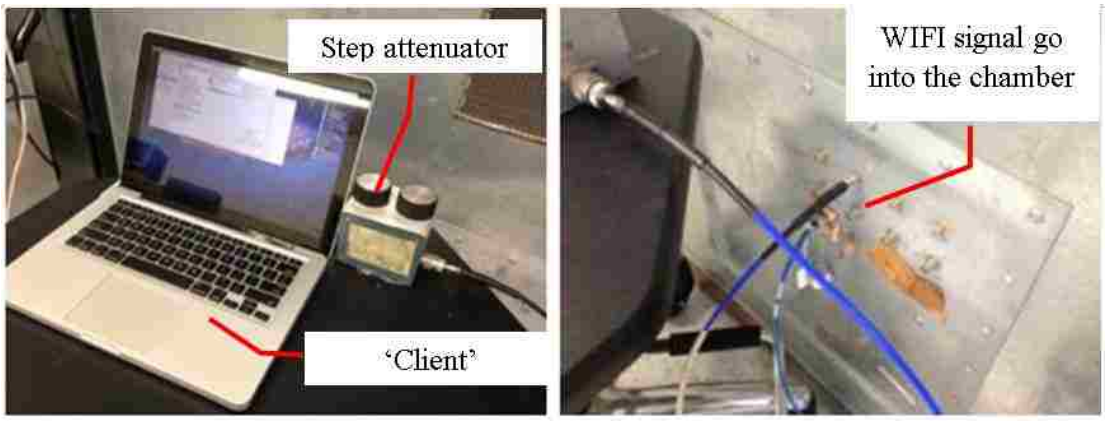

Figure 3.18 Setup outside the chamber

According to the RSSI, we could get the power present in a received Wi-Fi signal and compare the performance difference in the case of the same output power from the Wi-Fi signal. Several tools could monitor the RSSI of Wi-Fi signal, such as '802.11 Monitor' (Figure 3.19), that could monitor the RSSI for Wi-Fi different channels during the communication.

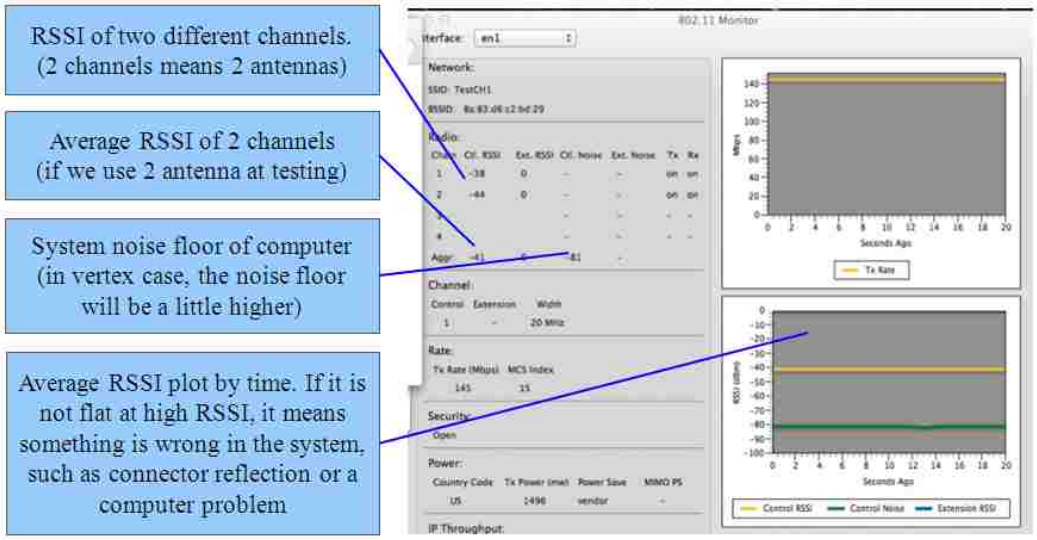

Figure 3.19 WIFI monitor software (802.11 Monitor)

As for the noise floor measurement, the laptop needs to work in a certain status to get the maximum noise from memory. We defined three cases for the laptop computer for the results comparison..

a) 'Idle' case: Close the applications in the laptop except OS, so there is less access to the memory card. We then get the smallest memory noise as a reference line.
b) 'Busy' case (vertex case): We run testing software called 'vertex', which forces the laptop to do a heavy calculation with continuous access of the memory card. This case gives the largest noise from memory.
c) 'Absorber Material' case: the laptop is run as in the 'Busy' case, but with a test piece of absorber material on the pins of the memory card.

The material position also on the memory pins (Figure 3.13), then measures the data rate at different Wi-Fi signal output levels using a step attenuator.

3.5.2. Measurement Steps. When the measurement setup has been prepared entirely, we performed the measurement as follows:

1) Set the display panel of the 'server' laptop to maximum angle in every measurement.
2) Build a Wi-Fi connection for a specific channel in the 'server' laptop.

3) Find and connect to this connection on the ‘client’ laptop.
4) Warm up the system for 0.5 h to make the whole system stable.
5) Run ‘iperf3’ and ‘802.11 monitor’, to put ‘server’ laptop into ‘server listening mode’.
6) Close all software on the ‘server’ computer except OS, terminal, and 802.11 monitor.
7) Make sure there is no absorber material in the ‘server’ computer.
8) Set step attenuator to 30 dB
9) Tighten all screws. Keep display brightness at 50%, close shielding door.
10) Record current RSSI.
11) Run ‘iperf3’ in ‘client’ laptop to start data transfer; after that, obtain data rate from ‘server’. This transfer processing will be performed three times automatically, so we can get three individual data rates.
12) Reduce attenuator by 2 dB steps and repeat steps (9) to (11) until the connection fails.
13) Run ‘vertex’; repeat step (7) to (12).
14) Open back cover of laptop and put a piece of the test material on the memory pins. Run ‘vertex’, then repeat steps (8) to (12), to obtain the material measurement results.
15) After all materials have been measured, repeat steps (7) to (13) to check the repeatability of the system.

3.5.3. Measurement Results and Discussion. Based on measurement results for three cases (idle, with vertex, material with vertex), we plotted the data rate value against the different RSSIs. (Figure 3.20). shows an example of a result plot for a material sample. From the results, when in ‘idle’ (blue curve), the Wi-Fi keeps working at lower signal power. In the ‘vertex’ case (without material) (red curve), the noise affected the wireless communication, so the data rate goes down at higher signal levels.

If using material on the memory pins, the minimal signal level could be increased around 6dB, meaning the material could improve the Wi-Fi communication sensitivity (pink curve).

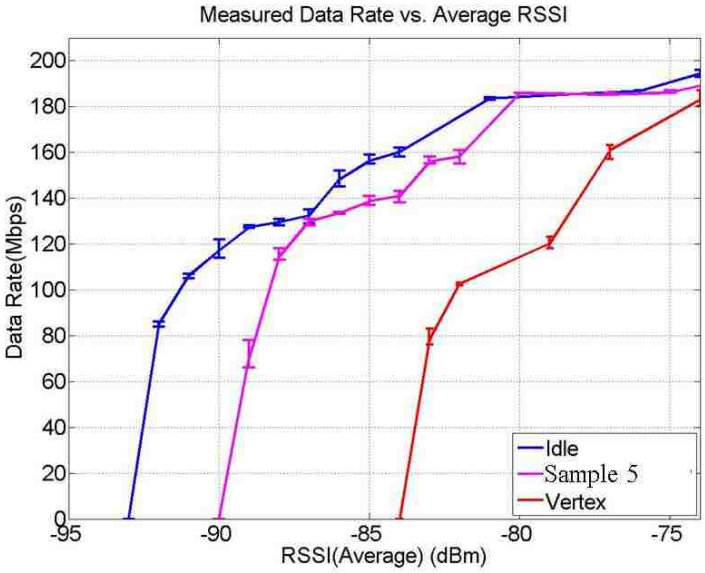

Figure 3.20 Example of data rate measurement results

3.6 RESULTS ANALYSIS

By the noise floor measurement, the EM noise from memory is significant in Wi-Fi/Bluetooth band when the laptop in the fully running condition. The inner Wi-Fi/Bluetooth antenna of laptop, which probably affects the wireless communication, measures the noise function. The noise is reduced around 5 dB when a piece of lossy absorbing material is put on the memory pins, as it improved the noise emission quantificationally. Due to the high-accuracy spectrum analyzer and preamplifier, the noise floor method could give stable and repeatable results for material performance.

Even if the EM noise exists and coupled to the Wi-Fi/Bluetooth antenna, it may not interfere with the laptop wireless system or worsen the wireless performance; in other words, the absorbing material has less value for this application. Therefore, the Wi-Fi communication method can directly tell the influence from absorbing materials for the wireless communication performance. The improvement of the data rate at both low-level signals and in the heavy load laptop running environment can help to find the most effective absorbing material for the customer.

The laptop-based evaluation method could reflect the performance of the absorbing material, and from the measurement of the same sample, the results from both

methods correlated well. This means the noise floor method can tell how much EMI is changed by the material and of how that material can help improve wireless function after evaluation using the second method.

4 CONCLUSIONS

In this thesis, firstly, we introduced a new kind of honeycomb panel consisting of a metal-coated plastic, and discussed the SE analysis and measurement for such a metal-coated honeycomb panel (MaxAir). For the second topic, we discussed how to evaluate lossy materials or sheet absorbers based on a laptop application to describe the instinctive performance of the material.

By the features of lower price, light weight, and easy to cut, the MaxAir honeycomb panel is suitable for many applications. SE is not only the most important parameter of MaxAir but is an important element when deciding its application. The nested reverb chamber method could provide an accurate and repeatable SE measurement for most honeycomb panels. According to the SE measurement results for different honeycomb samples, the SE of MaxAir is not as good as a traditional pure metal panel; numerical calculation confirmed this. Several factors would affect the SE performance of MaxAir during the measurement: the edge treatment is the most significant. Using fine copper wool could give the smallest leakage from the edges around the panel under test; therefore, the measured results reflect the actual SE performance of panel itself. In terms of results for different samples, the coating thickness and panel height determined the SE directly, and this agreed with shielding theory.

In the second topic, the internal Wi-Fi antenna of a laptop could detect the noise from the memory card connector through the noise measurement. Such noise appeared in the same frequency range as the Wi-Fi/Bluetooth band. The noise was reduced to some extent after putting lossy material on the memory connector; moreover, such a noise reduction would be different for individual material samples, which could be a good indicator for material performance. Furthermore, a Wi-Fi communication between laptops was built for the lossy material performance evaluation. The data rate changing in different Wi-Fi radiation levels directly tells of the effects from the lossy material. The data rate improvement agrees with the results from noise measurement very well. The laptop application based method proved an effective and instinctive evaluation method for lossy material

APPENDIX A.

MATLAB CODE FOR FREQUENCY STIRRING & SE RESULTS OF SAMPLES

The code is for the raw data post processing of frequency stirring mode in chapter 2 using MATLAB. SE measurement based on the nested reverb chamber method need the data of as many as possible frequency points, then do the zero-phase digital filtering by the following codes:

```
AvgNum = 100;            % Aeraging points number.
 [Ref_fAvg] = filterAvg(RefSE_L,AvgNum);   %  Filtering the Ref Data (without panel)
SampleSE_fAvg = 20*log10(SampleSE_fAvg);   % Turn processed Ref data to dB scale
[SampleSE_fAvg] = filterAvg(SampleSE_L,AvgNum); %  Filtering the measured Data (with panel sample)
SampleSE_fAvg = 20*log10(SampleSE_fAvg); % Turn processed Ref data to dB scale
SampleSE= Sample1SE_fAvg- SampleSE_fAvg; ; % SE results of current sample panel
```

In the above code, RefSE_L and SampleSE_L are the data directly from the measurement, they are correlated to the case of with and without honeycomb panel. They were converted to linear scale before the filtering processing. Doing the same processing for both data of with and without panel cases. After converting processed data to dB scale, the final SE results should be the deviation of without panel case and with panel case. For the zero-phase digital filtering processing, use the sub-function below:

```
function [fAvg] = filterAvg(data, aNum)

a=1;
b=1/aNum*ones(1,aNum);
fAvg=filtfilt(b,a,data);

end
```

The following plots show the shielding effectiveness results for all honeycomb panels from Laird, which measured in exactly same frequency range (1GHz to 20GHz) and

configuration. Considering the repeatability and uncertainty of measurement, use the best one of 2 times measurement as the final result for each panel.

Sample #	Name (core material)	Panel Thickness (inch)
1	Aluminum	0.5
2	Tubas 6 pcf PC	0.5
3	PEI 4 pcf	0.5
4	Tubas 10 pcf PC	0.5
5	Tubas 10 pcf PC	0.5
6	Tubas 10 pcf PC	0.5
7	Tubas 10 pcf PC	0.5
8	Aluminum	0.5
9	Aluminum	0.5
10	Tubas 6 pcf PC	0.25
11	Tubas 6 pcf PC	0.25
12	Tubas 6 pcf PC	0.5
13	Tubas 6 pcf PC	0.5
14	Tubas 6 pcf PC	0.25
15	Tubas 6 pcf PC	0.25
16	-	0.5
17	PEI 0.4	0.5
18	PEI 0.6	0.5
19	PEI 2	0.5
20	PEI 4	0.5
21	PEI 0.4	0.5
22	PEI 0.6	0.5
23	PEI 2	0.25
24	PEI 0.2	0.25

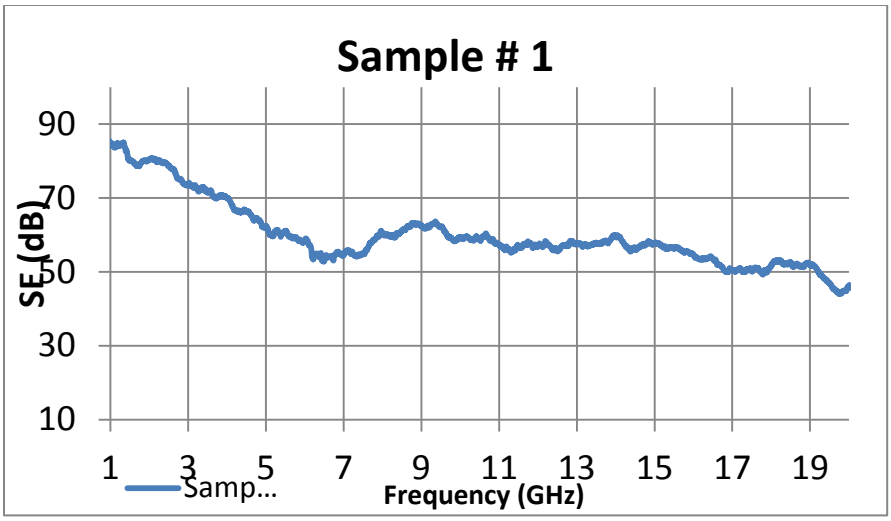
Sample # 1
90
70
50
30
10
SE (dB)
1
3
5
7
9
11
13
15
17
19
Samp...
Frequency (GHz)

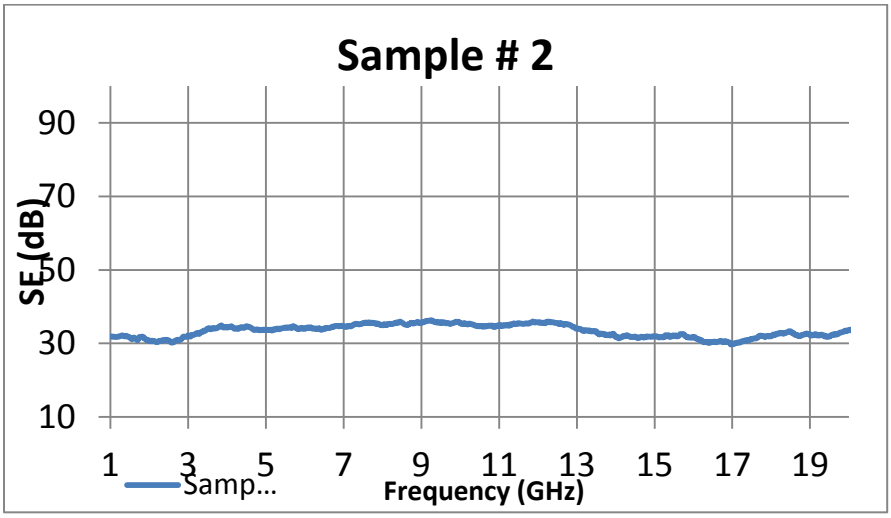
Sample # 2
90
70
50
30
10
SE (dB)
1
3
5
7
9
11
13
15
17
19
Samp...
Frequency (GHz)

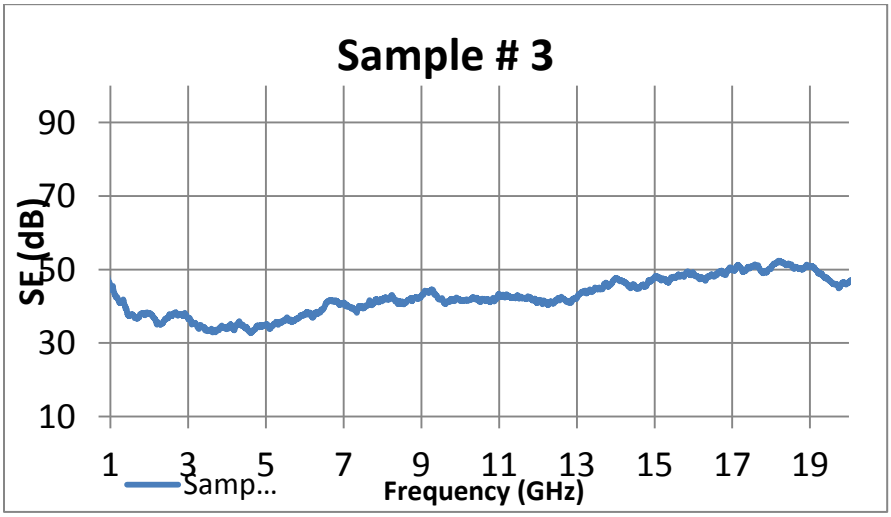
Sample # 3
90
70
50
30
10
SE (dB)
1
3
5
7
9
11
13
15
17
19
Samp...
Frequency (GHz)

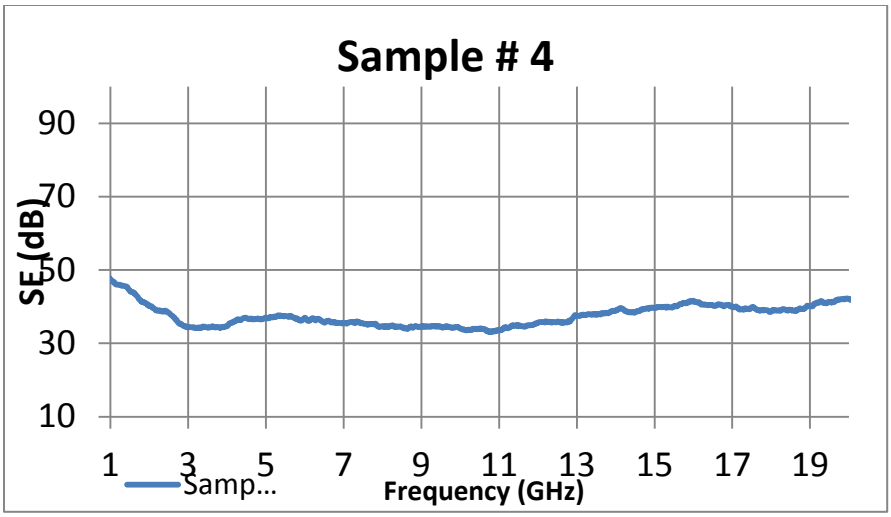
Sample # 4
90
70
50
30
10
SE (dB)
1
3
5
7
9
11
13
15
17
19
Frequency (GHz)
Samp...

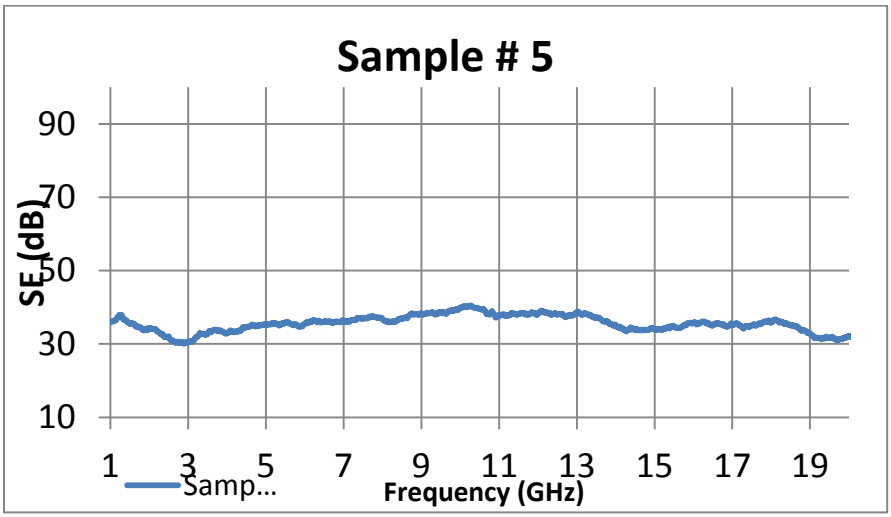
Sample # 5
90
70
50
30
10
SE (dB)
1
3
5
7
9
11
13
15
17
19
Frequency (GHz)
Samp...

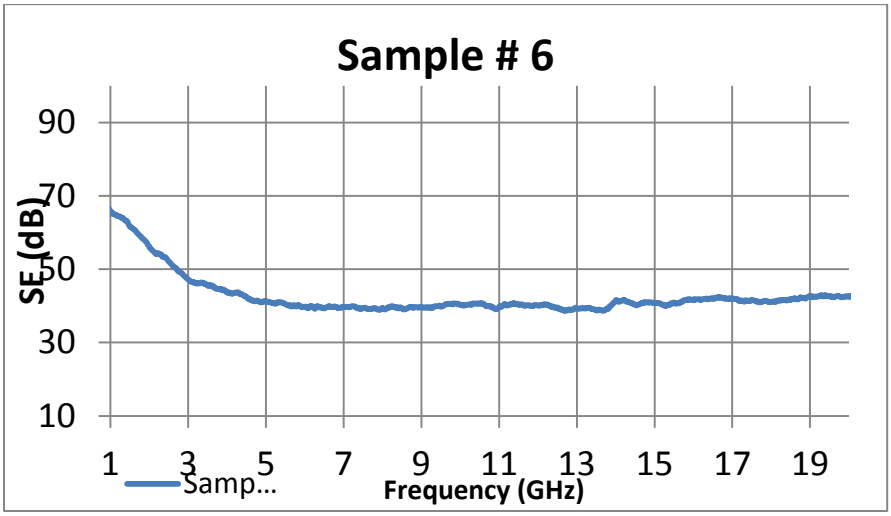
Sample # 6
90
70
50
30
10
SE (dB)
1
3
5
7
9
11
13
15
17
19
Frequency (GHz)
Samp...

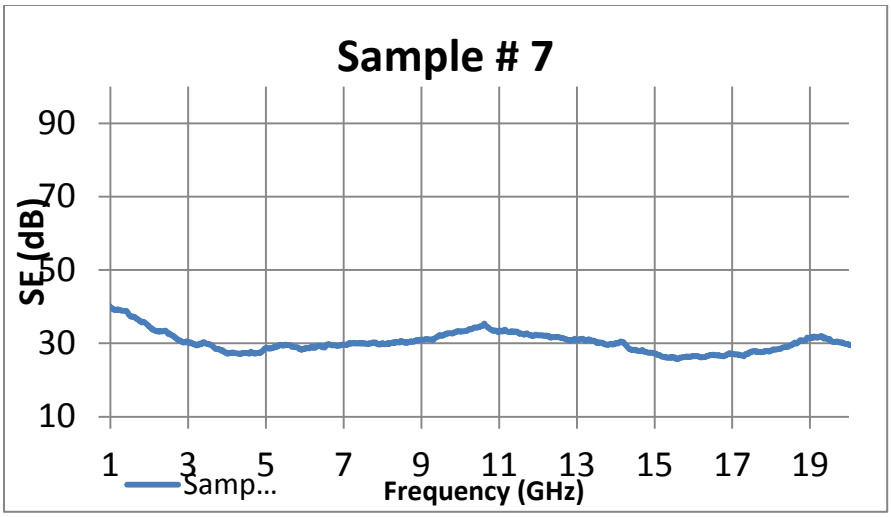
Sample # 7
90
70
50
30
10
SE (dB)
1
3
5
7
9
11
13
15
17
19
Frequency (GHz)
Samp...

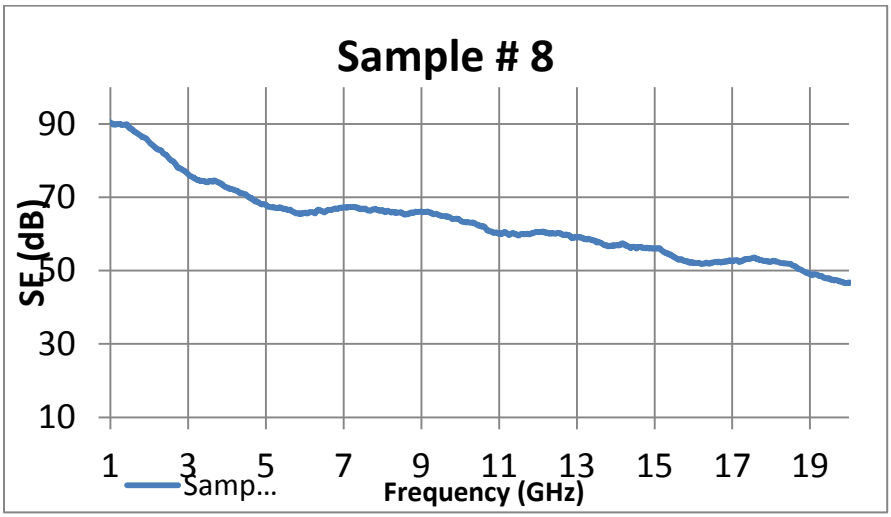
Sample # 8
90
70
50
30
10
SE (dB)
1
3
5
7
9
11
13
15
17
19
Frequency (GHz)
Samp...

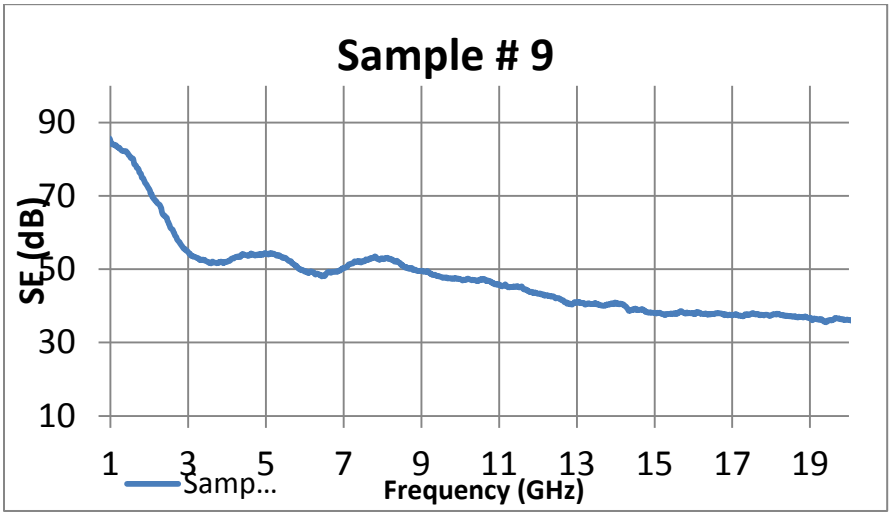
Sample # 9
90
70
50
30
10
SE (dB)
1
3
5
7
9
11
13
15
17
19
Frequency (GHz)
Samp...

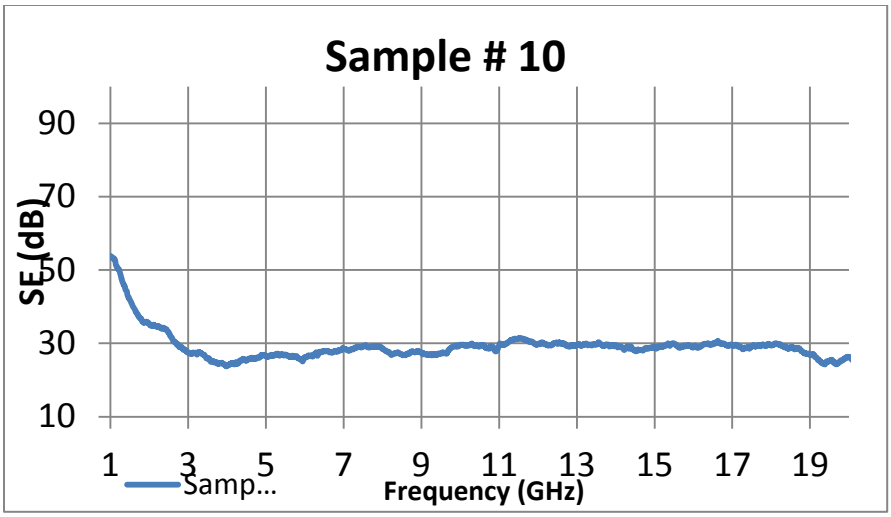
Sample # 10
90
70
50
30
10
SE (dB)
1
3
5
7
9
11
13
15
17
19
Frequency (GHz)
Samp...

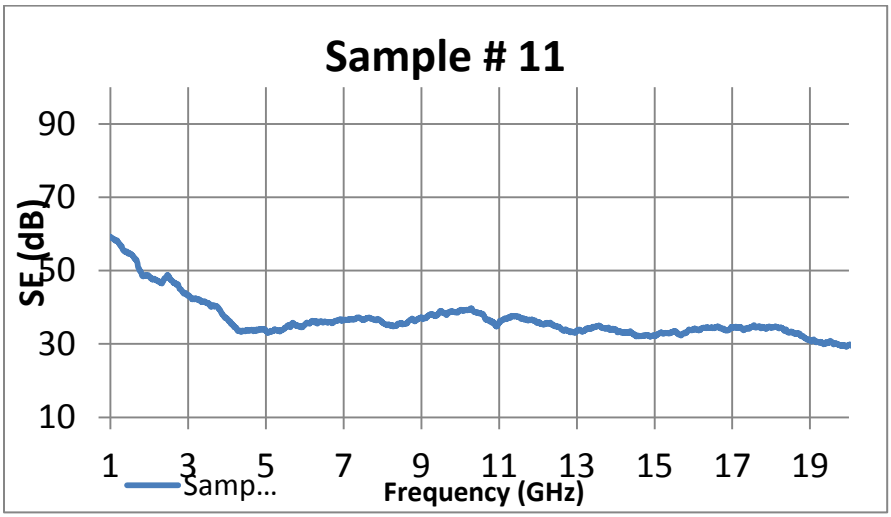
Sample # 11
90
70
50
30
10
SE (dB)
1
3
5
7
9
11
13
15
17
19
Frequency (GHz)
Samp...

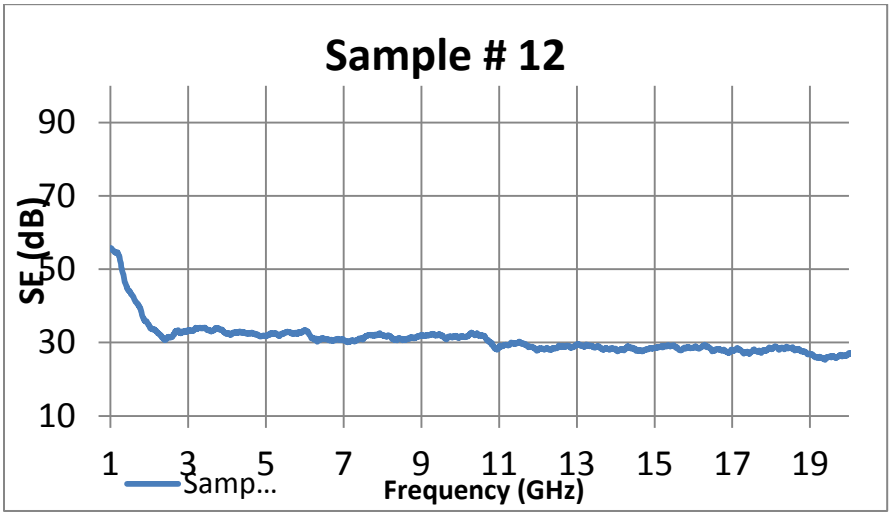
Sample # 12
90
70
50
30
10
SE (dB)
1
3
5
7
9
11
13
15
17
19
Frequency (GHz)
Samp...

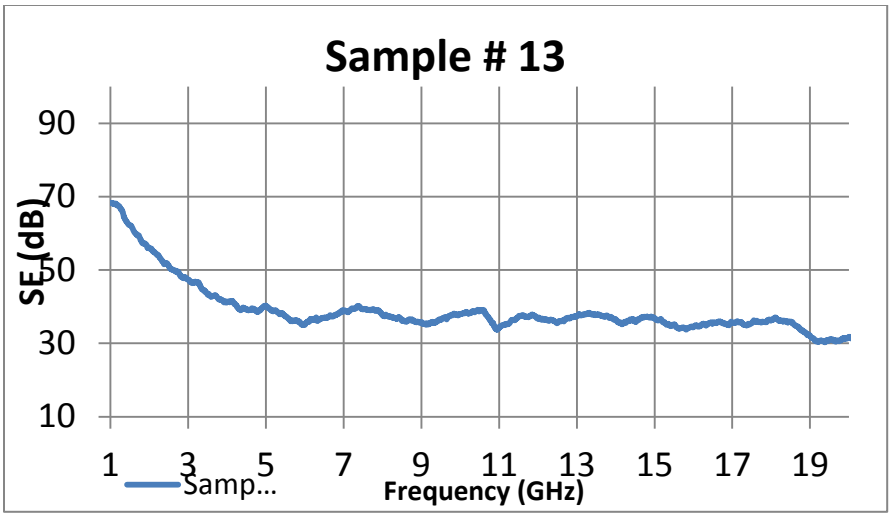
Sample # 13
90
70
50
30
10
SE (dB)
1
3
5
7
9
11
13
15
17
19
Frequency (GHz)
Samp...

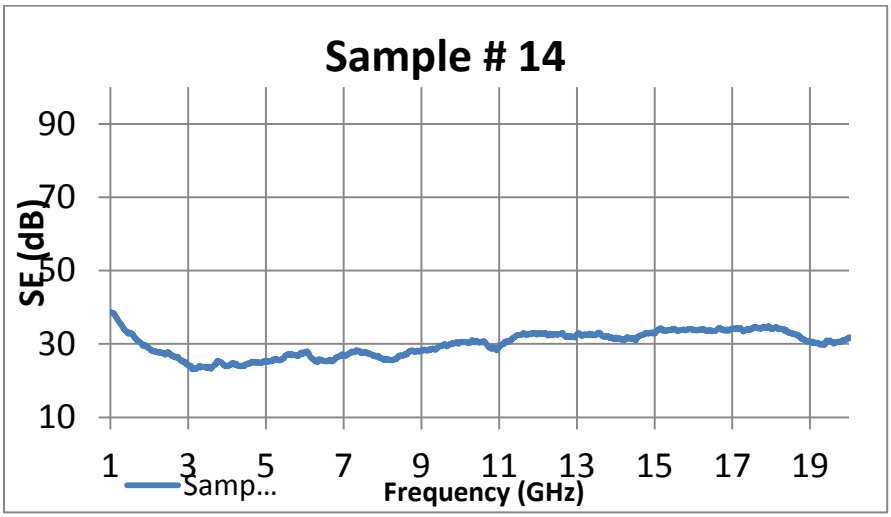
Sample # 14
90
70
50
30
10
SE (dB)
1
3
5
7
9
11
13
15
17
19
Frequency (GHz)
Samp...

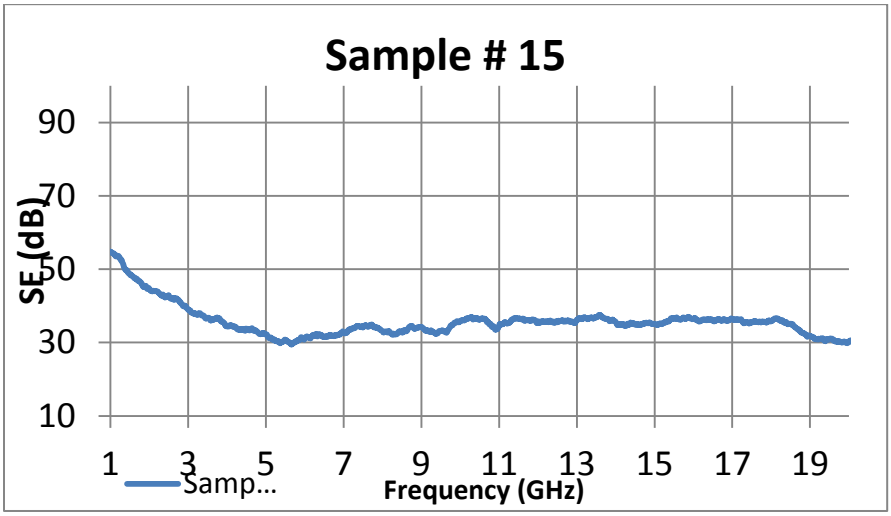
Sample # 15
90
70
50
30
10
SE (dB)
1
3
5
7
9
11
13
15
17
19
Frequency (GHz)
Samp...

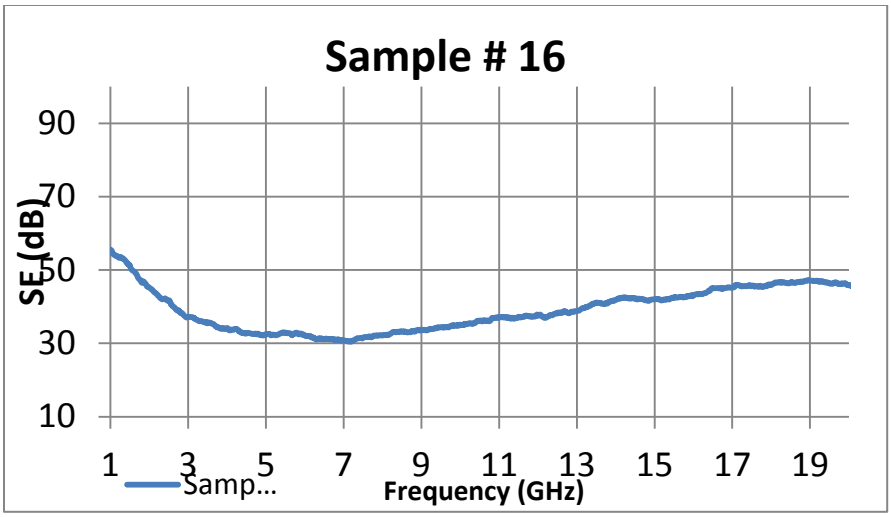
Sample # 16
90
70
50
30
10
SE (dB)
1
3
5
7
9
11
13
15
17
19
Samp...
Frequency (GHz)

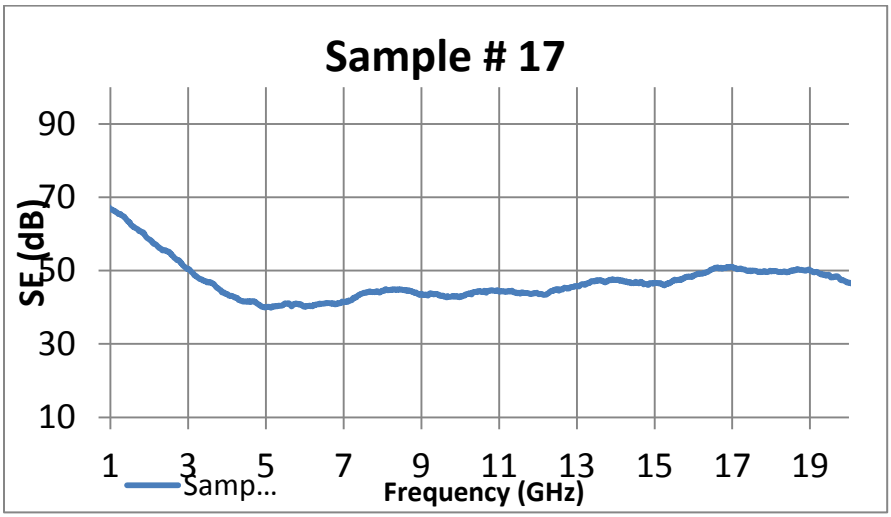
Sample # 17
90
70
50
30
10
SE (dB)
1
3
5
7
9
11
13
15
17
19
Samp...
Frequency (GHz)

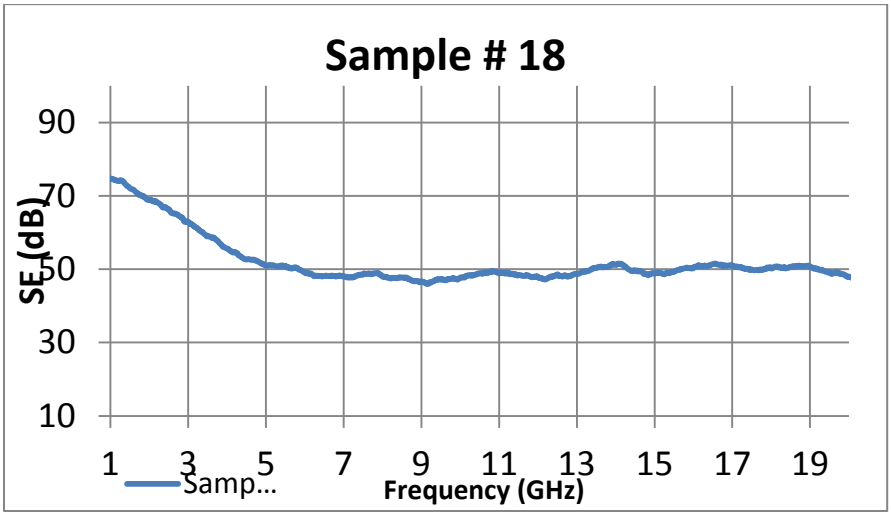
Sample # 18
90
70
50
30
10
SE (dB)
1
3
5
7
9
11
13
15
17
19
Samp...
Frequency (GHz)

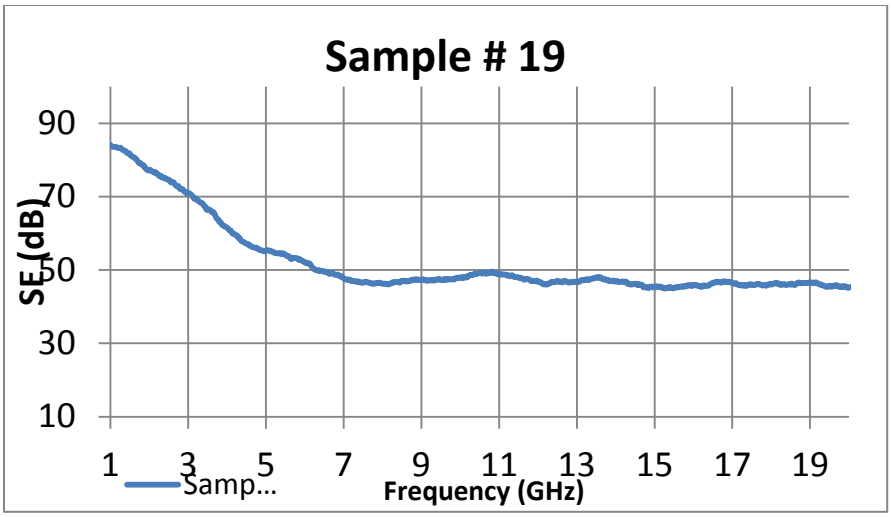
Sample # 19
90
70
50
30
10
SE (dB)
1
3
5
7
9
11
13
15
17
19
Samp...
Frequency (GHz)

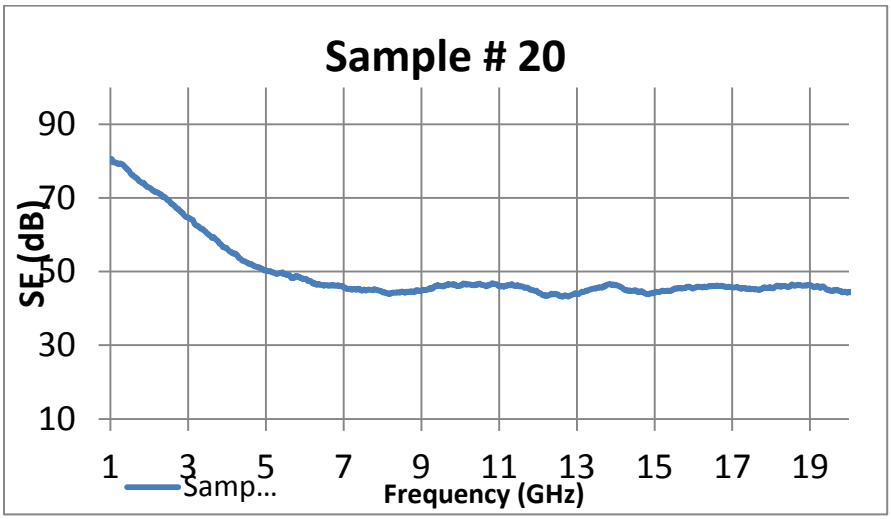
Sample # 20
90
70
50
30
10
SE (dB)
1
3
5
7
9
11
13
15
17
19
Samp...
Frequency (GHz)

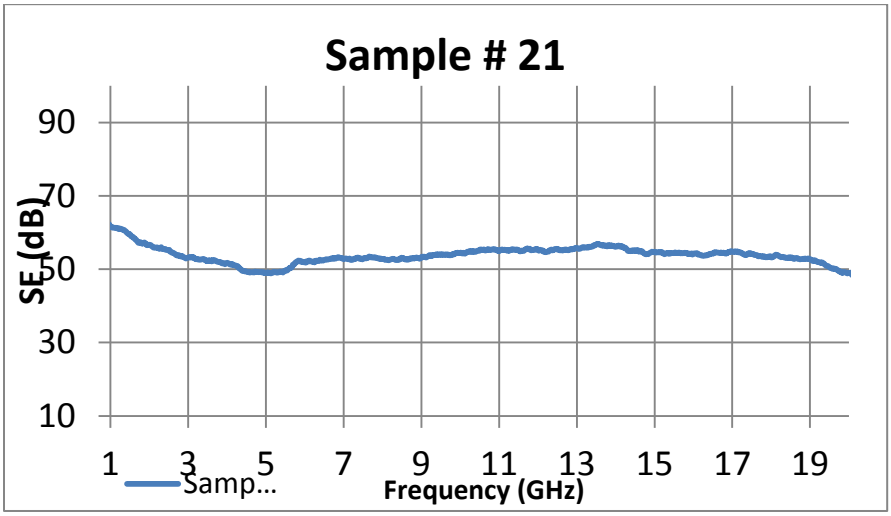
Sample # 21
90
70
50
30
10
SE (dB)
1
3
5
7
9
11
13
15
17
19
Samp...
Frequency (GHz)

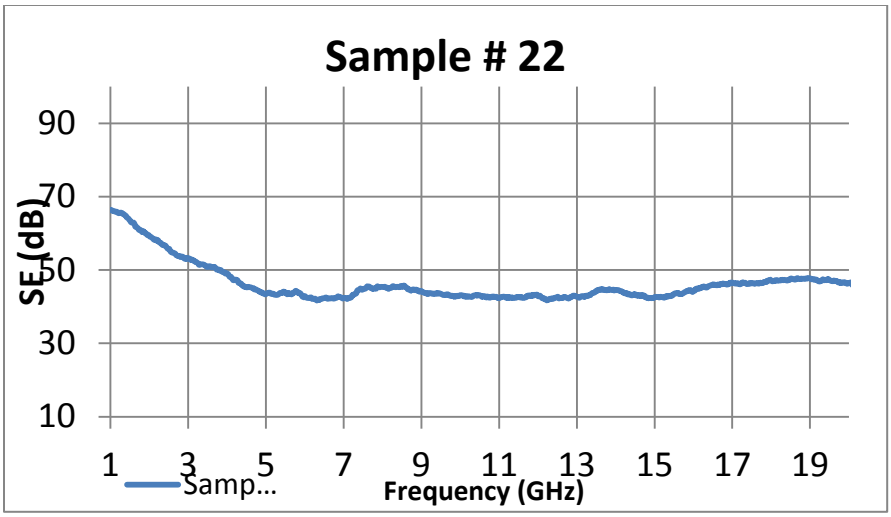
Sample # 22
90
70
50
30
10
SE (dB)
1
3
5
7
9
11
13
15
17
19
Frequency (GHz)
Samp...

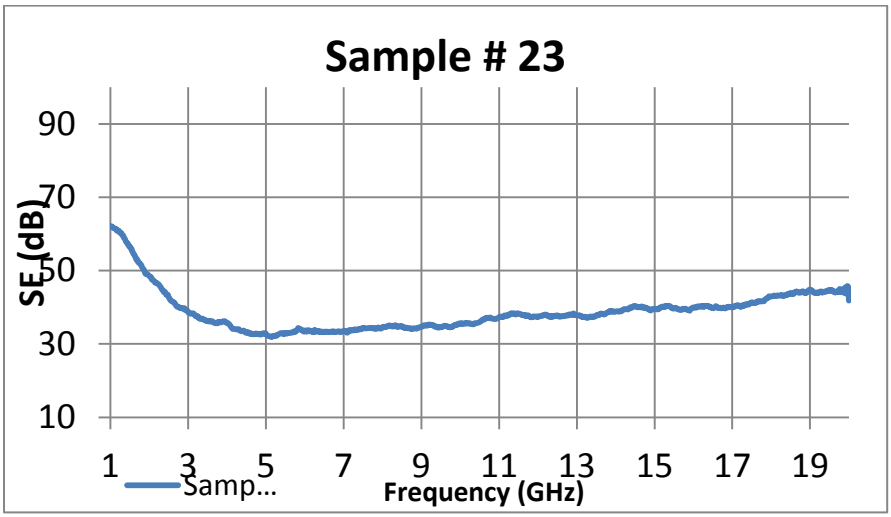
Sample # 23
90
70
50
30
10
SE (dB)
1
3
5
7
9
11
13
15
17
19
Frequency (GHz)
Samp...

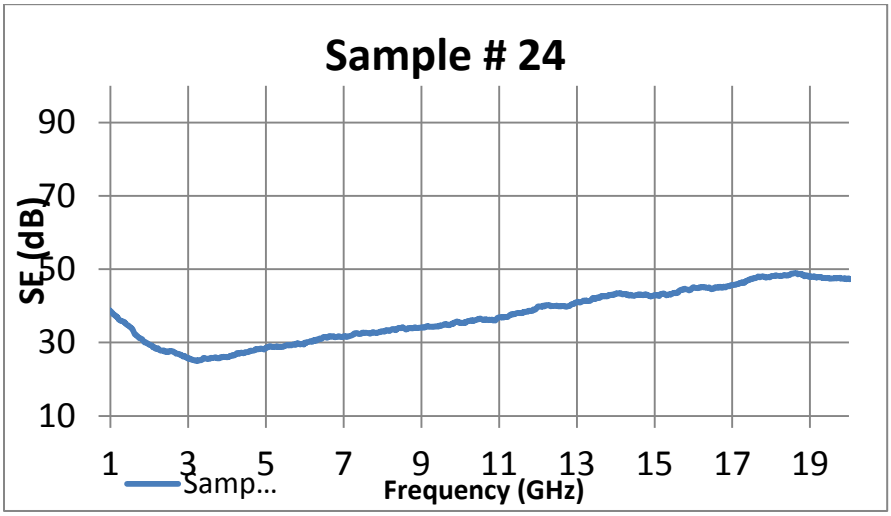
Sample # 24
90
70
50
30
10
SE (dB)
1
3
5
7
9
11
13
15
17
19
Frequency (GHz)
Samp...

APPENDIX B.

RESULTS OF ALL MATERIAL SAMPLES

As for the sheet absorbing material evaluation, noise floor measurement and data rate measurement results for all absorbing material as below:

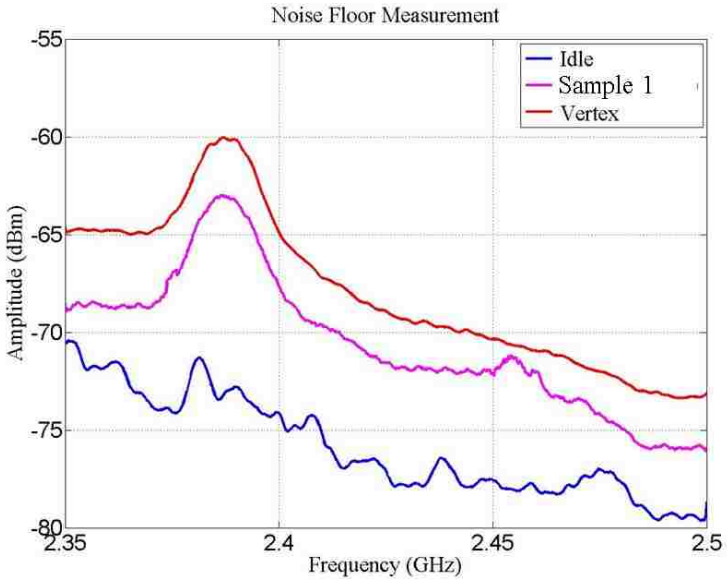

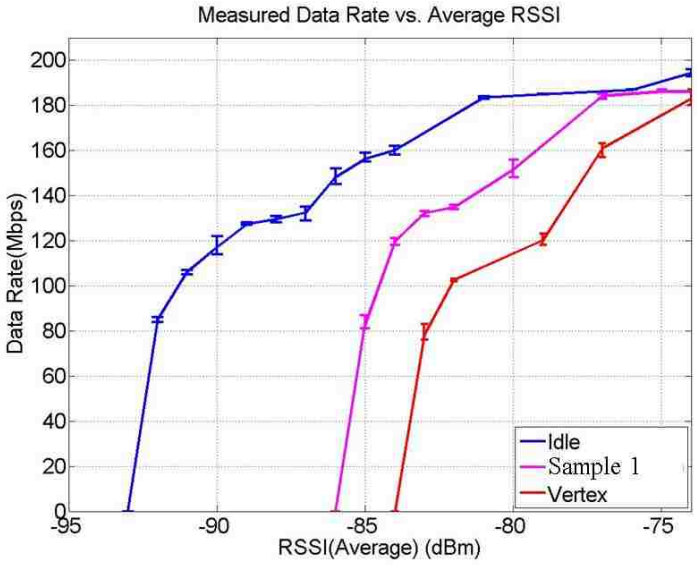

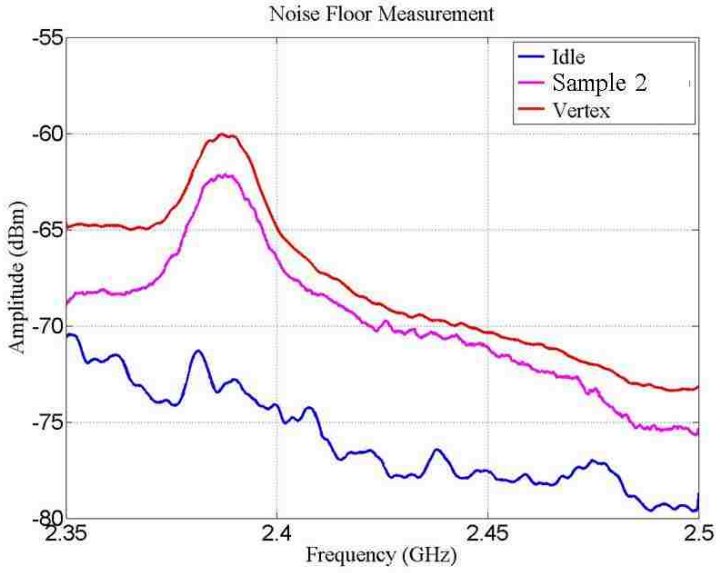
Noise Floor Measurement
Idle
Sample 2
Vertex
Amplitude (dBm)
-55
-60
-65
-70
-75
-80
2.35
2.4
2.45
2.5
Frequency (GHz)

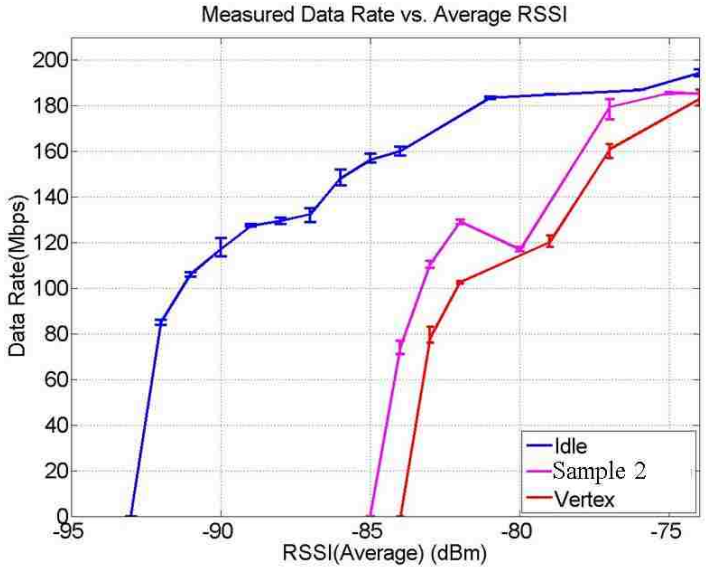
Measured Data Rate vs. Average RSSI
Data Rate(Mbps)
200
180
160
140
120
100
80
60
40
20
0
-95
-90
-85
-80
-75
RSSI(Average) (dBm)
Idle
Sample 2
Vertex

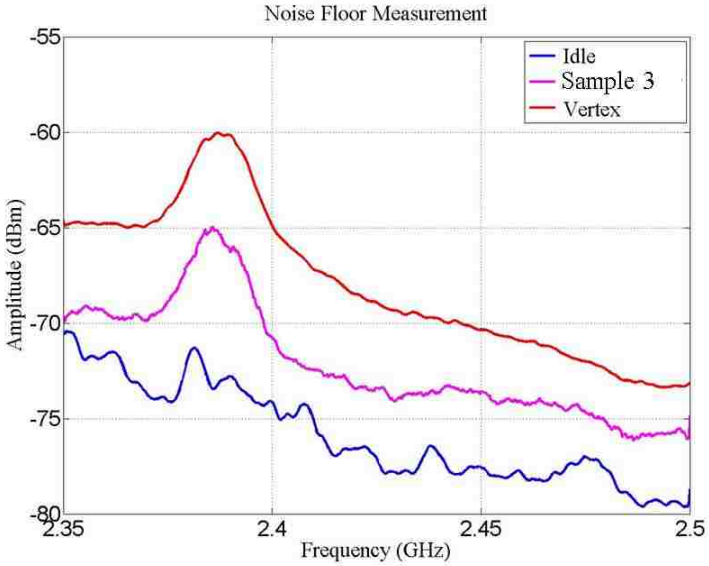
Noise Floor Measurement
Idle
Sample 3
Vertex
Amplitude (dBm)
-55
-60
-65
-70
-75
-80
2.35
2.4
2.45
2.5
Frequency (GHz)

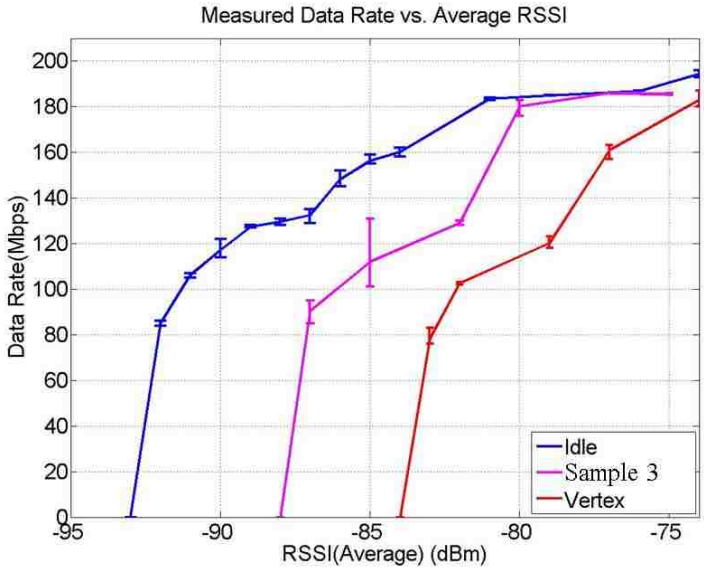
Measured Data Rate vs. Average RSSI
Data Rate(Mbps)
200
180
160
140
120
100
80
60
40
20
0
-95
-90
-85
-80
-75
RSSI(Average) (dBm)
Idle
Sample 3
Vertex

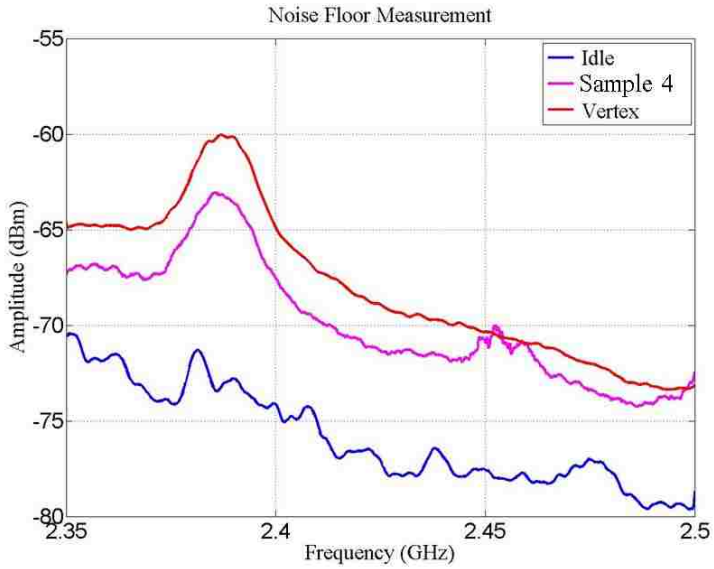
Noise Floor Measurement
Idle
Sample 4
Vertex
Amplitude (dBm)
-55
-60
-65
-70
-75
-80
2.35
2.4
2.45
2.5
Frequency (GHz)

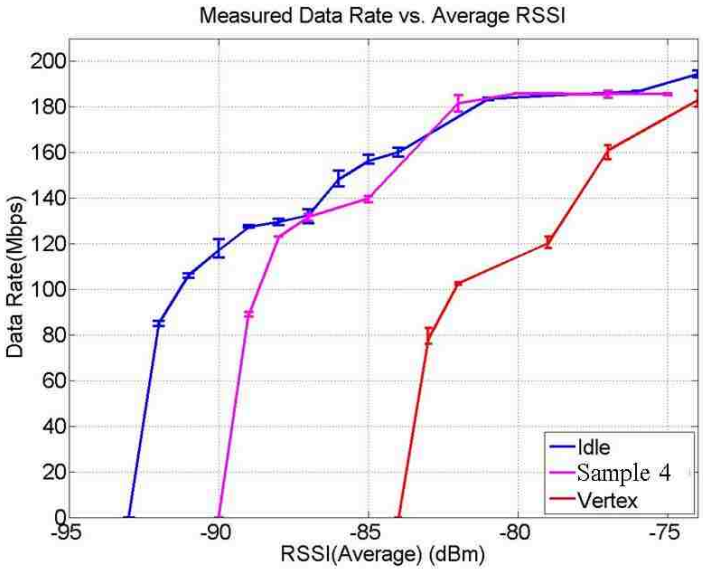
Measured Data Rate vs. Average RSSI
Data Rate(Mbps)
200
180
160
140
120
100
80
60
40
20
0
-95
-90
-85
-80
-75
RSSI(Average) (dBm)
Idle
Sample 4
Vertex

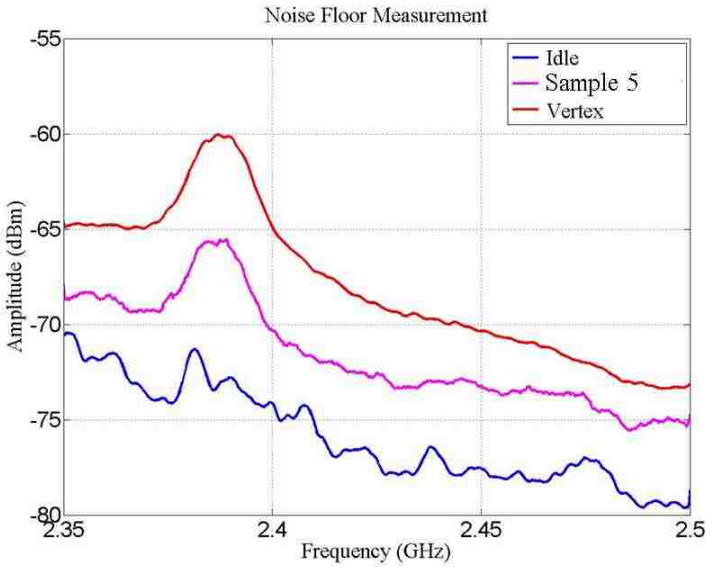
Noise Floor Measurement
Idle
Sample 5
Vertex
Amplitude (dBm)
-55
-60
-65
-70
-75
-80
2.35
2.4
2.45
2.5
Frequency (GHz)

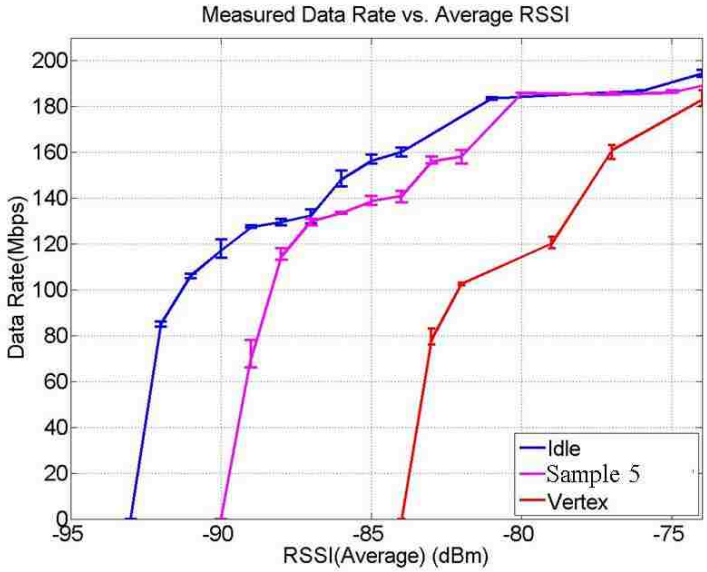
Measured Data Rate vs. Average RSSI
Data Rate(Mbps)
200
180
160
140
120
100
80
60
40
20
0
-95
-90
-85
-80
-75
RSSI(Average) (dBm)
Idle
Sample 5
Vertex

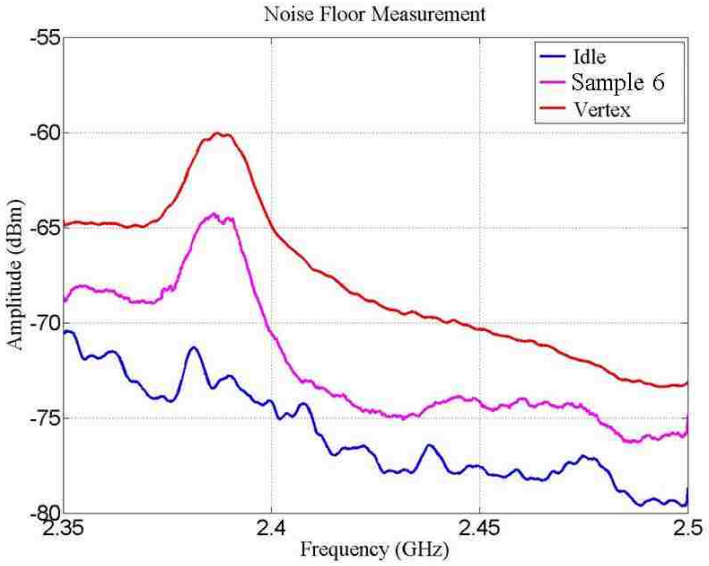
Noise Floor Measurement
Idle
Sample 6
Vertex
Amplitude (dBm)
-55
-60
-65
-70
-75
-80
2.35
2.4
2.45
2.5
Frequency (GHz)

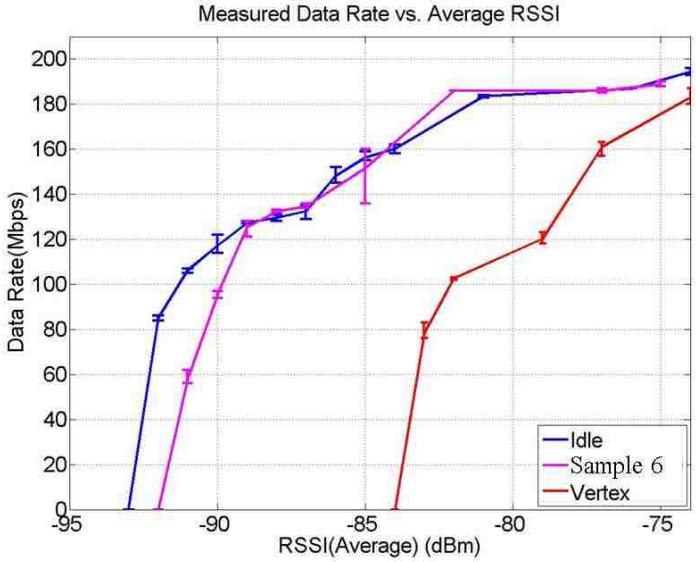
Measured Data Rate vs. Average RSSI
Data Rate(Mbps)
200
180
160
140
120
100
80
60
40
20
0
-95
-90
-85
-80
-75
RSSI(Average) (dBm)
Idle
Sample 6
Vertex

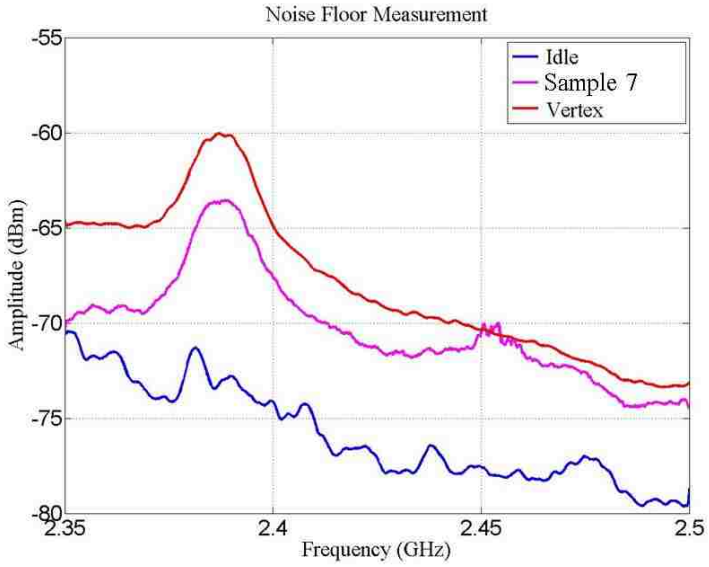
Noise Floor Measurement
Idle
Sample 7
Vertex
Amplitude (dBm)
-55
-60
-65
-70
-75
-80
2.35
2.4
2.45
2.5
Frequency (GHz)

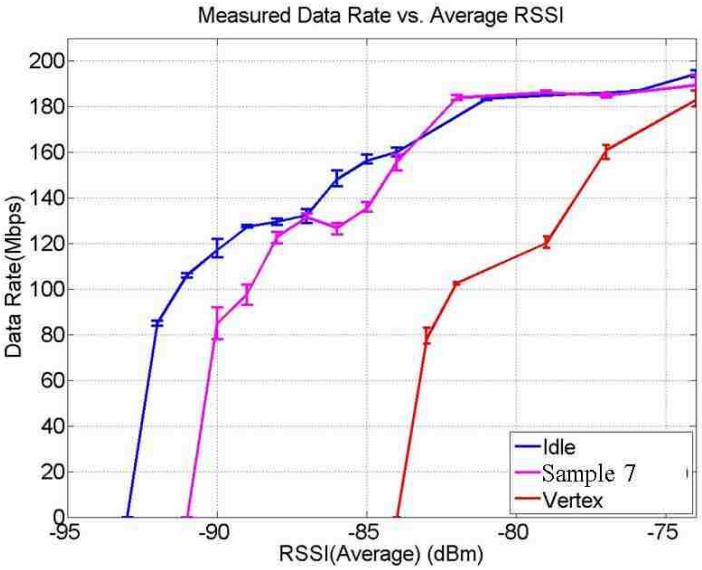
Measured Data Rate vs. Average RSSI
Data Rate(Mbps)
200
180
160
140
120
100
80
60
40
20
0
-95
-90
-85
-80
-75
RSSI(Average) (dBm)
Idle
Sample 7
Vertex

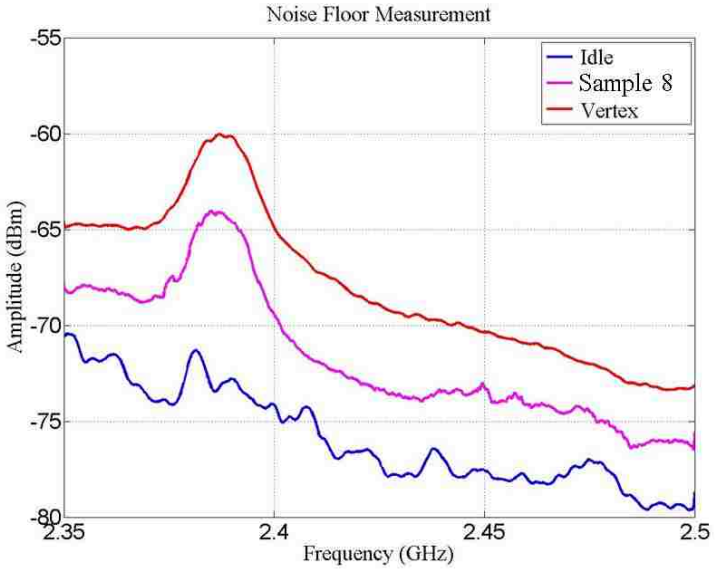
Noise Floor Measurement
Idle
Sample 8
Vertex
Amplitude (dBm)
-55
-60
-65
-70
-75
-80
2.35
2.4
2.45
2.5
Frequency (GHz)

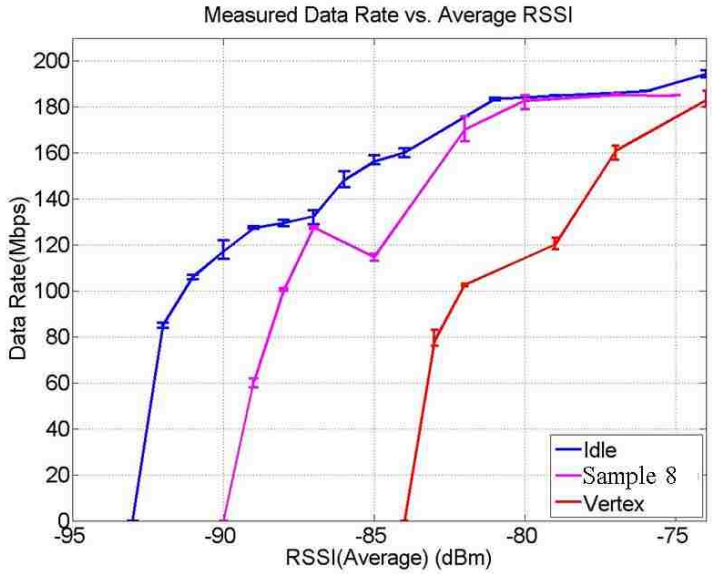
Measured Data Rate vs. Average RSSI
Data Rate(Mbps)
200
180
160
140
120
100
80
60
40
20
0
-95
-90
-85
-80
-75
RSSI(Average) (dBm)
Idle
Sample 8
Vertex

BIBLIOGRAPHY

[1] Donald R.J. White, Michel Mardiguian, "A Handbook Series on Electromagnetic Interference and Compatibility, Electromagnetic Shielding", *Interference Control Technologies, Inc*, Gainesville, Virginia pp 7.1-7.43.

[2] G. Fenical, "New Developments in Shielding Materials*", Systems, Applications and Technology Conference*, pp.1-5, 2006.

[3] R.Mittra, S.W.Lee, "Analytical Techniques in the Theory of Guided Waves", New York: MacMillan, pp.99-104, 1971.

[4] Folgueras, Mauro Angelo Alves, Mirabel Cerqueira Rezende, "Dielectric properties of microwave absorbing sheets produced with silicone and polyaniline", *Mat.Res*, vol.13 2010.

[5] Kyung-Won Lee, Yeong-Chul Cheong, Ic-Pyo Hong and Jong-Gwan Yook. "Design Equation of Shielding Effectiveness of Honeycomb", *PROCEEDINGS OF ISAP2005*, SEOUL, KOREA, 2005.

[6] Bereuter, W.A, Chang, D, "Shielding Effectiveness of Metallic Honeycombs", *IEEE Transactions on EMC*, 1982.

[7] IEEE 299.1, "IEEE Draft Standard Method for Measuring the Shielding Effectiveness of Enclosures and Boxes Having All Dimensions between 0.1 m and 2 m ", 2011.

[8] Christopher L. Holloway, David A. Hill, John Ladbury, Galen Koepke, and R. Garzia, "Shielding Effectiveness Measurements of Materials Using Nested Reverberation Chambers", *IEEE Transactions on EMC*, Vol. 45, NO. 2, 2003.

[9] M. O. Hatfield, "Shielding effectiveness measurements using mode-stirred chambers: a comparison of two approaches," *IEEE Transactions on EMC*, vol. 30, 1988.

[10] W. Kurner, A. Schwab, "Parameters and results of SE-measurements performed in mode-stirred chambers," in *Proc. 2000 IEEE International Symposium EMC*, 2000.

[11] Andrew C Marvin, Yuhui He, "A Study of Enclosure Shielding Effectiveness Measurement using Frequency Stirring in a Mode-Stirred Chamber", *EMC 2008. IEEE International Symposium*, 2008.

[12] Marina Y. Koledintseva, Jianfeng Xu, "Systematic Analysis and Engineering of Absorbing Materials Containing Magnetic Inclusions for EMC Applications", *IEEE Transactions on Magnetics*, 2011.

[13] M. Koledintseva, K.N. Rozanov, and J. Drewniak, "Engineering, modeling and testing of composite absorbing materials for EMC applications", *Advances in Composite Materials - design and Analysis*, 2011.

[14] Jing Li, Yao-Jiang Zhang, "EMI Reduction Evaluation with Flexible Absorbing Materials and Ferrite Cores Applied on Cables", *IEEE International Symposium on EMC*, 2012.

[15] Randy Bancroft, "A commercial Perspective on the Development and Integration of and 802.11 a/b/g HiperLan/WLAN Antenna into Laptop Computers", *Antennas and Propagation Magazine, IEEE* Vol. 48, 2006.

[16] Giuliano Manzi, Mauro Feliziani, Pierre A. Beeckman and Nico van Dijk, "Coexistence between Ultra-Wideband Radio and Narrow-Band Wireless LAN Communication Systems—Part II: EMI Evaluation", *IEEE Transactions on EMC*, Vol. 51, 2009.

[17] Bruce Archambeault, Samuel Connor, "Measurements and Simulations for Ground-to-Ground Plane Noise DDR RAM Daughter Cards and Motherboards for EM1 Emissions", *IEEE International Symposium on EMC*, Vol. 1, 2002.

[18] Andriy Radchenko, Joseph Bishop, Richard Johnson, Paul Dixon, Marina Koledintseva, "Sheet Absorbing Material Modeling and Application for Enclosures", *IEEE International Symposium on EMC*, 2013.

[19] L.F. Chen, C.K. Ong, C.P. Neo, V.V. Varadan, and V.K. Varadan, "Microwave Electronics: Measurement and Materials Characterization", *Wiley, Hoboken*, 2004.

VITA

Xiao Li was born in Beijing, China. In November 1982, he obtained his Bachelor Degree from Beijing Information Technology University in Electric Engineering, Beijing, China. In June 2001, he obtained his Master Degree from Beijing Jiaotong University in Electric Communication Engineering. In March 2008.

In June 2012, he enrolled at the Missouri University of Science and Technology to pursue his Master's Degree in Electrical Engineering, during which time he was a graduate research assistant in Electromagnetic Compatibility Laboratory. From May 2013 to May 2014, he did internship at Cisco Systems, San Jose, CA. He received his Master's Degree in August 2014.